Remote Sensing of Environment 145 (2014) 154–172

Contents lists available at ScienceDirect

Remote Sensing of Environment

journal homepage: www.elsevier.com/locate/rse

Landsat-8: Science and product vision for terrestrial global change research

D.P. Roy [a,*], M.A. Wulder [b], T.R. Loveland [c], C.E.Woodcock [d], R.G. Allen [e], M.C. Anderson [f], D. Helder [g], J.R. Irons [h], D.M. Johnson [i], R. Kennedy [d], T.A. Scambos [j], C.B. Schaaf [k], J.R. Schott [l], Y. Sheng [m], E.F. Vermote [n], A.S. Belward [o], R. Bindschadler [p], W.B. Cohen [q], F. Gao [r], J.D. Hipple [s], P. Hostert [t], J. Huntington [u], C.O. Justice [v], A. Kilic [w], V. Kovalskyy [a], Z.P. Lee [k], L. Lymburner [x], J.G. Masek [y], J. McCorkel [y], Y. Shuai [z], R. Trezza [e], J. Vogelmann [c], R.H. Wynne [aa], Z. Zhu [d]

[a] Geographic Information Science Center of Excellence, South Dakota State University, Brookings, SD 57007, USA
[b] Canadian Forest Service (Pacific Forestry Centre), Natural Resources Canada, 506 West Burnside Road, Victoria, British Columbia, V8Z 1M5, Canada
[c] U.S. Geological Survey Earth Resources Observation and Science (EROS) Center 47914 252nd Street, Sioux Falls, SD 57198, USA
[d] Department of Earth and Environment, Boston University, MA 02215, USA
[e] University of Idaho Research and Extension Center, Kimberly, ID 83341, USA
[f] United States Department of Agriculture, Agricultural Research Service, Hydrology and Remote Sensing Laboratory, Beltsville, MD 20705, USA
[g] College of Engineering, South Dakota State University Brookings, SD 57007, USA
[h] Laboratory for Atmospheres, NASA Goddard Space Flight Center, Greenbelt, MD 20771, USA
[i] United States Department of Agriculture, National Agricultural Statistics Service, 3251 Old Lee Highway, suite 305, Fairfax, VA 22030, USA
[j] National Snow and Ice Data Center, University of Colorado, 1540 30th Street, Boulder CO 80303, USA
[k] School for the Environment, University of Massachusetts Boston, Boston, MA 02125, USA
[l] Rochester Institute of Technology, Chester F. Carlson Center for Imaging Science, Rochester, NY 14623, USA
[m] Department of Geography, University of California, Los Angeles (UCLA), Los Angeles, CA 90095, USA
[n] Terrestrial Information Systems Laboratory, NASA Goddard Space Flight Center, Greenbelt, MD, 20771, USA
[o] European Commission, Joint Research Centre, Institute for Environment and Sustainability, 20133 VA, Italy
[p] Hydrospheric and Biospheric Sciences Laboratory, NASA Goddard Space Flight Center, Greenbelt, MD 20771, USA
[q] USDA Forest Service, PNW Research Station, Corvallis, OR 97331, USA
[r] USDA Agricultural Research Service, Hydrology and Remote Sensing Laboratory, Beltsville, MD 20705, USA
[s] United States Department of Agriculture, Risk Management Agency, Washington, DC 20250, USA
[t] Geography Department, Humboldt-Universität zu Berlin, Unter den Linden 6, 10099 Berlin, Germany
[u] Desert Research Institute, Reno, NV, 89501, USA
[v] Department of Geographical Sciences, University of Maryland, College Park, MD 20742, USA
[w] Dept. of Civil Engineering, School of Natural Resources, University of Nebraska-Lincoln, Lincoln, NE 65816, USA
[x] Geoscience Australia, GPO Box 378 Canberra ACT 2601, Australia
[y] Biospheric Sciences Laboratory, NASA Goddard Space Flight Center, Greenbelt, MD 20771, USA
[z] ERT Inc. at the Biospheric Sciences Laboratory of NASA's Goddard Space Flight Center, Greenbelt, MD 20771, USA
[aa] Virginia Tech, Forest Resources and Environmental Conservation, 310 West Campus Dr, Blacksburg, VA 24061, USA

ARTICLE INFO

Article history:
Received 9 October 2013
Received in revised form 28 January 2014
Accepted 1 February 2014
Available online 4 March 2014

Keywords:
Landsat 8
OLI
TIRS
Landsat Science Team

ABSTRACT

Landsat 8, a NASA and USGS collaboration, acquires global moderate-resolution measurements of the Earth's terrestrial and polar regions in the visible, near-infrared, short wave, and thermal infrared. Landsat 8 extends the remarkable 40 year Landsat record and has enhanced capabilities including new spectral bands in the blue and cirrus cloud-detection portion of the spectrum, two thermal bands, improved sensor signal-to-noise performance and associated improvements in radiometric resolution, and an improved duty cycle that allows collection of a significantly greater number of images per day. This paper introduces the current (2012–2017) Landsat Science Team's efforts to establish an initial understanding of Landsat 8 capabilities and the steps ahead in support of priorities identified by the team. Preliminary evaluation of Landsat 8 capabilities and identification of new science and applications opportunities are described with respect to calibration and radiometric characterization; surface reflectance; surface albedo; surface temperature, evapotranspiration and drought; agriculture; land cover, condition, disturbance and change; fresh and coastal water; and snow and ice. Insights into the development of derived 'higher-level' Landsat products are provided in recognition of the growing need for consistently processed, moderate spatial resolution, large area, long-term terrestrial data records for resource management and for climate and global change studies. The paper concludes with future prospects, emphasizing the opportunities for land

* Corresponding author.

http://dx.doi.org/10.1016/j.rse.2014.02.001

imaging constellations by combining Landsat data with data collected from other international sensing systems, and consideration of successor Landsat mission requirements.

1. Introduction

At over 40 years, the Landsat series of satellites provides the longest temporal record of space-based surface observations. Landsat 1 was launched in 1972 and was followed by a series of consecutive, temporally overlapping, Landsat observatories (Landsat 2, 3, 4, 5 and 7) that have provided near-global coverage reflective and thermal wavelength observations with increasing spectral and spatial fidelity (Lauer, Morain, & Salomonson, 1997; Loveland & Dwyer, 2012; Williams, Goward, & Arvidson, 2006). Remarkably, the Landsat record is unbroken, with most land locations acquired at least once per year since 1972, capturing a period when the global human population has more than doubled (United Nations Population Division, 2011) and evidence for climate change has become discernible (Hansen, Sato, & Ruedy, 2012; IPCC, 2013). Landsat data offer a unique record of the land surface and its modification over time. The Landsat moderate spatial resolution is sufficiently resolved to enable chronicling of anthropogenic and natural change at local to global scale (Gutman et al., 2008; Townshend & Justice, 1988) and the data time series are calibrated to provide a characterized consistent record (Markham & Helder, 2012) that is needed to enable discrimination between data artifacts and actual land surface temporal changes (Roy et al., 2002). Landsat data have demonstrated capabilities for mapping and monitoring of land cover and land surface biophysical and geophysical properties (Hansen & Loveland, 2012; Wulder, Masek, Cohen, Loveland, & Woodcock, 2012) and potential utility for terrestrial assimilation and biogeochemical cycling and land use forecasting applications (Lewis et al., 2012; Nemani et al., 2009; Sleeter et al., 2012). Applications addressed with Landsat data involve both scientific discovery and managing and monitoring resources for economic and environmental quality, public health and human well-being, and national security. Analyses of the economic benefits of Landsat vary from $935 million/year (ASPRS, 2006) to $2.19 billion/year (Miller, Richardson, Koontz, Loomis, & Koontz, 2013) in support of applications including water resource analysis and management, agriculture and forest analysis and management, homeland security, infrastructure analysis, disaster management, climate change science, wetland protection, and monitoring land cover change.

The 40 + year Landsat record was continued with the successful February 11th 2013 launch of Landsat 8 from Vandenburg Air Force Base, California. This new Landsat observatory was developed through an interagency partnership between the National Aeronautics and Space Administration (NASA) and the Department of the Interior U.S. Geological Survey (USGS) (Irons & Loveland, 2013). NASA led the mission and was responsible for system engineering and design, developing the flight segment, securing launch services, flight ground systems integration, and conducting on-orbit initialization and verification. NASA referred to the effort as the Landsat Data Continuity Mission (LDCM) during the development, launch, and on-orbit commissioning. USGS led the ground system development and the LDCM was renamed Landsat 8 on May 30th 2013 when the USGS formally took responsibility for mission operations, including collecting, archiving, processing, and distributing Landsat 8 data. Landsat 8 carries two sensors, the Operational Land Imager (OLI) and the Thermal Infrared Sensor (TIRS), and over 500 image scenes per day are ingested into the U.S. Landsat data archive at the USGS Earth Resource Observation and Science (EROS) Center, South Dakota. The new Landsat 8 scenes complement the now more than four million scenes acquired by previous Landsat missions that are stored in the U.S. Landsat archive and are freely available via the internet (Woodcock et al., 2008).

This paper introduces the current (2012–2017) USGS–NASA Landsat Science Team (LST) efforts to establish an initial understanding of Landsat 8 capabilities and the steps ahead in support of science team identified priorities. These priorities and the purpose and focus of the current LST are first introduced. This is followed by an overview of the Landsat 8 mission objectives, sensors, orbit, data acquisition, and standard data products to provide context for the subsequent sections. Preliminary evaluation of Landsat 8 capabilities and identification of new science and applications opportunities are highlighted, followed by insights into the development of derived 'higher-level' Landsat products, international synergies between Landsat and other moderate resolution remote sensing satellites, and a conclusion that includes consideration of successor Landsat mission requirements.

2. Landsat 8 Science Team

This paper is authored by members and affiliates of the current LST. There have been several LSTs, each selected through a competitive proposal review process to serve a five-year term funded by the USGS and/or NASA. The science teams were charged to provide feedback on critical design issues, including functional performance specifications of the Landsat instruments, data systems and data formats that affect Landsat data users, and to consider interoperability of Landsat with other planned and in orbit remote sensing systems, and to provide insights on future missions. The previous LST (2005–2011) provided justification for making the U.S. Landsat data archive available at no cost, recommended strategies for the effective expansion and use of the archived Landsat data, and investigated the requirements for Landsat 8 to meet the needs of users including policy makers (Woodcock et al., 2008; Wulder & Masek, 2012). The LST prior to that (1996–2001) was formulated as part of the Landsat 7 development phase in a period when Landsat 5 was the only operating Landsat due to the 1993 Landsat 6 failure (Goward et al., 2006; Irons & Masek, 2006). It developed a Landsat 7 long-term data acquisition plan, undertook research to develop methods to analyze Landsat data for global change studies, and evaluated the data quality acquired by Landsat 7 after it was launched in April 1999 (Arvidson, Gasch, & Goward, 2001; Goward, Masek, Williams, Irons, & Thompson, 2001).

The current LST (2012–2017) was selected with an aim to represent the breadth of Landsat user perspectives and their requirements. The LST is comprised of 21 principal investigator-lead teams of scientists and engineers drawn from academia, U.S. Federal science and mission agencies, and includes representation from non-U.S. institutions to ensure an international perspective. The majority of the science team members have expertise in processing and characterizing Landsat data and/or expertise using Landsat data for a specific application domain. The LST met prior to and shortly after Landsat 8 launch and established the following four core priorities for the next five years:

(1) evaluation of Landsat 8 capabilities and identification of new science and applications opportunities,
(2) development of strategies and prototype approaches for the development of 'higher-level' derived Landsat science products needed in support of global change research,
(3) identification of international land imaging constellation opportunities,
(4) definition of science and applications requirements for succeeding Landsat missions for operational long-term observational continuity.

Section 4 of this paper focuses on the first priority, which is most immediate and is described in the hierarchy of processing required to transform Landsat 8 data into derived products and provide core applications. Sections 5 and 6 reflect current LST perspectives on the second and third priorities respectively as they are evolving. The conclusion includes consideration of successor Landsat mission requirements.

3. Landsat 8 overview

3.1. Mission objectives

The primary Landsat 8 mission objective is to extend the Landsat record into the future and maintain continuity of observations so that Landsat 8 data are consistent and comparable with those from the previous Landsat systems. Landsat supports the global data and information needs of the NASA Earth Science program, which seeks to develop a scientific understanding of the Earth system and its response to natural and human-induced changes to enable improved prediction of climate, weather, and natural hazards (Irons, Dwyer, & Barsi, 2012; NRC, 2007). The Landsat legacy has been relatively consistent in mission objectives, with capabilities modified by incremental improvements in satellite, sensor, transmission, reception, data processing, and data distribution technologies. Landsat currently provides an integral role in NASA's multi-scale global observing strategy. Notably, the NASA Terra satellite was placed in the same morning orbit as Landsat 7 to provide opportunities for multi-scale global land surface change monitoring (Skole, Justice, Janetos, & Townshend, 1997), particularly using data from the Moderate Resolution Imaging Spectroradiometer (MODIS) and the Advanced Spaceborne Thermal Emission and Reflection Radiometer (ASTER) that include Landsat heritage spectral bands (Justice et al., 1998; Yamaguchi, Kahle, Tsu, Kawakami, & Pniel, 1998). Landsat also supports the national data and information needs of the USGS national science strategy (USGS, 2007) and USGS initiatives such as the U.S. National Land Cover Database (Fry et al., 2011) that are reliant on the U.S. Landsat data coverage.

Landsat 8 is a science mission, and as for the previous Landsat systems, has no operational mandate (Wulder, White, Masek, Dwyer, & Roy, 2011). Specifically, this means that if the current Landsat 8 system fails there will be no quick replacement with another Landsat. The development of the Landsat 8 mission is reviewed in Irons et al. (2012). In 2005 NASA began planning for a free-flyer government-only Landsat 7 successor mission with the following objectives (Irons et al., 2012):

(a) collect and archive moderate-resolution, reflective multispectral image data affording seasonal coverage of the global land mass for a period of no less than five years;
(b) collect and archive moderate-resolution, thermal multispectral image data affording seasonal coverage of the global land mass for a period of no less than three years;
(c) ensure that the data are sufficiently consistent with data from the earlier Landsat missions, in terms of acquisition geometry, calibration, coverage characteristics, spectral and spatial characteristics, output product quality, and data availability, to permit studies of land cover and land use change over multi-decadal periods;
(d) distribute standard data products on a nondiscriminatory basis and at no cost to users.

These four objectives, the lessons learned from the Earth Observing-1 mission that demonstrated the advantages and challenges associated with a multispectral optical wavelength pushbroom sensor (Ungar, Pearlman, Mendenhall, & Reuter, 2003), and recommendations from the previous Landsat Science Teams provided the basis for the Landsat 8 capabilities and performance specifications that are summarized in the remainder of this Section.

3.2. Landsat 8 sensor overview

The Landsat 8 satellite carries a two-sensor payload, the Operational Land Imager (OLI) and the Thermal Infrared Sensor (TIRS), which are described in detail in Irons et al. (2012) and are summarized in Table 1. The OLI and TIRS spectral bands remain broadly comparable to the Landsat 7 Enhanced Thematic Mapper plus (ETM+) bands. Compared to the ETM+, the OLI has two additional reflective wavelength bands: a new shorter wavelength blue band (0.43–0.45 μm) intended for improved sensitivity to chlorophyll and other suspended materials in coastal waters and for retrieving atmospheric aerosol properties, and a new shortwave infrared band (1.36–1.39μm) for cirrus cloud detection. The other OLI bands are spectrally narrower in most cases than the corresponding ETM+ bands. In particular, the OLI near-infrared (NIR) band is closer in width to the MODIS NIR band and avoids the 0.825 μm water vapor absorption feature that occurs in the ETM+ NIR band. The TIRS senses emitted radiance in two 100 m thermal infrared bands, compared to the high and low gain single thermal infrared 60 m ETM+ band. The reduced TIRS spatial resolution is not optimal but was necessitated by engineering cost restrictions. However, the two thermal TIRS bands enable thermal wavelength atmospheric correction and more reliable retrieval of surface temperature and emissivity.

The OLI and TIRS designs incorporate technical advancements that improve their performance over the previous Landsat sensors. Significantly, like the Advanced Land Imager (ALI) on EO-1, both the OLI and TIRS are pushbroom sensors with focal planes aligning long arrays of detectors across-track. This provides improved geometric fidelity, radiometric resolution and signal-to-noise characteristics (Irons et al., 2012) compared to the whisk-broom sensor technology used by previous Landsat instruments (Lee, Storey, Choate, & Hayes, 2004) and by MODIS (Wolfe et al., 2002). The OLI band signal-to-noise ratios exceed those achieved by the Landsat ETM+ by a factor of at least eight (Irons et al., 2012). These improvements enable the OLI and TIRS analog-to-digital converters to quantize the sensed radiance into 12 bits (4096 levels) of meaningful data, rather than the 8 bits (256 levels) used by Landsat ETM+. The greater 12-bit quantization permits improved measurement of subtle variability in surface conditions. Calibration coefficients for all Landsat sensors are configured to globally maximize the range of land surface radiance in each spectral band (Markham, Goward, Arvidson, Barsi, & Scaramuzza, 2006). The dynamic range of the OLI is improved compared to previous Landsat sensors, reducing band saturation over highly reflective surfaces such as snow or cloud.

3.3. Landsat 8 orbit and data acquisition

The Landsat 8 satellite is in the same near-polar, sun-synchronous, 705 km circular orbit and position as the recently decommissioned Landsat 5 satellite. Landsat 8 data are acquired in 185 km swaths and segmented into 185 km × 180 km scenes defined in the second World-wide Reference System (WRS-2) of path (groundtrack parallel) and row (latitude parallel) coordinates also used by the Landsat 4, 5, and 7 satellites (Arvidson et al., 2001). Landsat 8 has a 16 day repeat cycle; each WRS-2 path/row is overpassed every 16 days and may be acquired a maximum of 22 or 23 times per year, as for Landsat 4, 5 and 7. Combined, the Landsat 8 and 7 sensors provide the capability to acquire any WRS-2 path/row every 8 days at the Equator and more frequent coverage at higher latitudes due to the poleward convergence of the Landsat orbits (Kovalskyy & Roy, 2013).

The amount of Landsat data in the U.S. Landsat archive has not been constant among Landsat sensors, from year to year, or geographically, because of differing Landsat data acquisition strategies, data reception capabilities, and system health issues (Goward et al., 2006; Loveland & Dwyer, 2012; Markham, Storey, Williams, & Irons, 2004). Landsat 7 was the first Landsat mission that adopted a systematic acquisition plan in 1999, and Landsat 7 data continue to be acquired systematically

Table 1
Comparison of Landsat 8 Operational Land Imager (OLI) and Thermal Infrared Sensor (TIRS) bands with the Landsat 7 Enhanced Thematic Mapper Plus (ETM+) bands.

Landsat 8		Landsat 7	
Band description (30 m native resolution unless otherwise denoted)	Wavelength (μm)	Band description (30 m native resolution unless otherwise denoted)	Wavelength (μm)
Band 1 — blue	0.43–0.45		
Band 2 — blue	0.45–0.51	Band 1 — blue	0.45–0.52
Band 3 — green	0.53–0.59	Band 2 — green	0.52–0.60
Band 4 — red	0.64–0.67	Band 3 — red	0.63–0.69
Band 5 — near infrared	0.85–0.88	Band 4 — near infrared	0.77–0.90
Band 6 — shortwave infrared	1.57–1.65	Band 5 — shortwave infrared	1.55–1.75
Band 7 — shortwave infrared	2.11–2.29	Band 7 — shortwave infrared	2.09–2.35
Band 8 — panchromatic (15 m)	0.50–0.68	Band 8 — panchromatic (15 m)	0.52–0.90
Band 9 — cirrus	1.36–1.38		
Band 10 — thermal Infrared (100 m)	10.60–11.19	Band 61 — thermal Infrared (60 m)	10.40–12.50 (high gain)
Band 11 — thermal Infrared (100 m)	11.50–12.51	Band 62 — thermal Infrared (60 m)	10.40–12.50 (low gain)

in an attempt to refresh annually the U.S. Landsat archive with sunlit, substantially cloud-free acquisitions that capture seasonal land surface dynamics (Arvidson, Goward, Gasch, & Williams, 2006). Globally, outside of the conterminous United States, however, only a fraction of the potential Landsat 7 WRS-2 path/rows are acquired (Arvidson et al., 2006; Ju & Roy, 2008).

The Landsat 8 data acquisition plan seeks to directly benefit global studies by acquiring the majority of the land WRS-2 paths/rows overpassed each day. The Landsat 8 satellite has improved high capacity onboard recording and satellite to ground transmission capabilities compared to previous Landsat systems. The data are transmitted via X-band to three primary ground receiving stations located at Gilmore Creek in Alaska, Svalbard in Norway, and at the USGS Earth Resource Observation and Science (EROS) Center in the U.S. International cooperator receiving stations, typically national space and mapping agencies, may receive real time Landsat 8 data transmissions within line-of sight of the satellite. Unlike previous Landsat missions, all of the Landsat 8 data available to the international cooperator receiving stations are stored and transmitted directly to the primary ground receiving stations and added to the U.S Landsat archive (Loveland & Dwyer, 2012). Approximately 60% more Landsat 8 scenes are acquired per day compared to Landsat 7. This improved data acquisition provides near-global seasonal coverage and the possibility to generate global Landsat data sets with adjacent cloud-free path/rows acquired only months apart, particularly if combined with data from other contemporaneous Landsat and Landsat-like sensors (Kovalskyy & Roy, 2013).

3.4. Landsat 8 Level 1 data product

Landsat 8 data are nominally processed into 185 km × 180 km Level 1 terrain-corrected (L1T) products that have a typical 950 MB compressed GeoTiff file size — more than twice that of previous Landsat sensor L1T products. All the OLI and TIRS spectral bands are stored as geolocated 16-bit digital numbers in the same L1T file. The 100 m TIRS bands are resampled by cubic convolution to 30 m and co-registered with the 30 m OLI spectral bands. An associated metadata file stores spectral band gain and offset numbers that can be used to linearly convert the digital numbers to at-sensor radiance ($W\,m^{-2}\,sr^{-1}\,\mu m^{-1}$) and to convert the OLI digital numbers to at-sensor reflectance (unitless). In this way users do not need to perform the non-linear transformation from radiance to reflectance which can be challenging for less experienced users (Roy et al., 2010). The Landsat 8 L1T product also provides a spatially explicit data quality assessment file that indicates the probability of clouds defined using a supervised classification algorithm (Scaramuzza, Bouchard, & Dwyer, 2012), terrain occlusion, and the presence of dropped data for each 30 m pixel location. The L1T products are defined in the Universal Transverse Mercator (UTM) map projection with World Geodetic System 84 (WGS84) datum to be compatible with heritage Landsat data, including Landsat 1–5 Multi-Spectral Scanner (MSS) data (Tucker, Grant, & Dykstra, 2004). The L1T data for Antarctica are defined in the Polar Stereographic projection to reduce polar map projection distortions.

The Landsat 8 L1T data processing includes radiometric calibration, systematic geometric correction, precision correction assisted by ground control chips, and the use of a digital elevation model to correct parallax error due to local topographic relief (Lee et al., 2004; Storey, Lee, & Choate, 2008). The radiometric calibration approach is described in Section 4. The Landsat 8 L1T products have improved geometric fidelity because of the Landsat 8 pushbroom sensor design and because the satellite has a fully operational onboard global positioning system (GPS) to measure the exterior orientation directly, rather than inferring it from ground control chips as with previous Landsat geolocation algorithms. Geolocation accuracy is improved, particularly in regions of unstructured and featureless terrain and over cloudy WRS-2 path/rows where ground control chip availability is normally reduced (Roy et al., 2010; Wolfe et al., 2002). The Landsat 8 L1T product has a 90% confidence level OLI to TIRS co-registration uncertainty requirement of <30 m, which is needed for applications that use both the reflective and emitted radiance, and a circular geolocation error uncertainty requirement of <12 m (Irons et al., 2012). These geometry improvements will enable more accurate mapping and monitoring applications, the generation of less smoothed temporally composited Landsat 8 data products (Roy, 2000), and more accurate multi-temporal change detection (Townshend, Justice, Gurney, & McManus, 1992).

4. Preliminary Landsat science team evaluation of Landsat 8 capabilities and identification of new science and applications opportunities

4.1. Calibration and radiometric characterization

Prior to launch, the OLI and TIRS were subject to rigorous pre-launch testing and measurements to characterize their radiometric, spectral, spatial and environmental parameters (Markham et al., 2008; Thome et al., 2011). This knowledge is used to provide the relationship between the at-sensor radiance ($W\,m^{-2}\,sr^{-1}\,\mu m^{-1}$) and the digital numbers output for each pixel and each spectral band. Also pre-launch, NASA and the European Space Agency (ESA) performed a national laboratory traceable cross-calibration comparison of the OLI and the Landsat-like multi-spectral instrument (MSI) that will be on the Sentinel-2 satellites (ESA, 2013) to ensure that their data will be cross-calibrated.

Calibration and radiometric characterization is included as a LST activity because of the post-launch degradation that can occur in the relationship between the at-sensor radiance and the recorded digital numbers, and the need to ensure consistency with archived Landsat data. On-board Landsat 8, calibration is undertaken every orbit; the TIRS radiometric response is examined by consideration of deep space

and on-board blackbody observations, and the OLI response is examined by observations of on-board solar diffuser panels. Due to the rigors of launch and the harsh space environment, on-board calibration is supplemented with vicarious techniques that use ground-based measurements to predict sensor outputs (Schott et al., 2012; Slater et al., 1987). For Landsat 8 a suite of globally distributed well-characterized sites based on previous Landsat vicarious calibration studies are being used (Helder et al., 2013). Other sensors will be cross-calibrated with Landsat 8 by comparison of near-simultaneous sensor observations over these sites. In addition, Landsat 8 vicarious calibration is being undertaken by sensing the moon, which is a known target with minimal atmospheric contamination (Kieffer et al., 2003), and will be used to detect long-term sensor degradations.

Shortly after launch the Landsat 8 orbit was configured to under-fly Landsat 7 to provide a vicarious cross-calibration opportunity. The Landsat 7 ETM + calibration is well defined, with 5% absolute reflective band calibration uncertainty (Markham & Helder, 2012) and thermal band uncertainties of approximately 0.6 K when expressed as a change in apparent temperature of a 300 K surface (Schott et al., 2012). During the under-flight, contemporaneous ground-based measurements were made continuously for four days. In addition, an airborne sensor package consisting of a hyperspectral imager, lidar, and thermal camera made measurements over several sites (McCorkel, Thome, & Lockwood, 2013).

Together, these pre-launch, onboard and vicarious calibration techniques established confidence in Landsat 8 calibration accuracy and continuity with predecessor Landsats. Initial results indicate absolute calibration within the pre-launch specification OLI requirements of 3% reflectance and 5% radiance (Czapla-Myers, Anderson, & Biggar, 2013; Markham, Irons, & Storey, 2013). Currently the TIRS data show an approximate 2% (band 10) and 4% (band 11) bias in absolute radiance when compared to vicarious measurements from buoys in Lake Tahoe, the Salton Sea, and deep oceans. This bias translates to an approximately 2 K to 4 K over estimate when expressed as a change in the apparent temperature of a 300 K surface and exceeds the 2% accuracy requirements for TIRS. Stray light from beyond the nominal 15° TIRS field of view has been identified as the cause of the bias and a correction approach is being studied. Until these studies produce a more comprehensive correction, the USGS plans to reprocess Landsat 8 data and subtract 0.29 $W/m^2/sr/um$ from TIRS band 10 and 0.51 $W/m^2/sr/um$ from TIRS band 11 to improve the accuracy of the data products for surface temperatures typical of mid-latitudes during the growing season, that is, temperatures near the 280 K to 300 K range of the buoy observations. On-orbit assessments also indicate that OLI and TIRS meet their geometric performance requirements with wide margins, giving confidence that their data can be readily incorporated into the Landsat time series (Markham et al., 2013).

4.2. Surface reflectance

The spectral bidirectional surface reflectance, i.e., derived top of atmosphere (TOA) reflectance corrected for the varying scattering and absorbing effects of atmospheric gases and aerosols is needed to monitor the surface reliably (Kaufman, 1989). Although the OLI's spectral bands are narrow and chosen to avoid atmospheric absorption features (Section 3.2), atmospheric effects are still challenging to correct. In particular, the impact of aerosols can be difficult to correct because of their complex scattering and absorbing properties that vary spectrally and with the aerosol size, shape, chemistry and density (Dubovik et al., 2002). A number of atmospheric correction methodologies have been developed, but those using radiative transfer algorithms and atmospheric characterization data provide the most potential for automated large-area application (Vermote, El Saleous, & Justice, 2002; Roy et al., 2014). For example, the MODIS reflective wavelength bands have been atmospherically corrected using the 6SV radiative transfer code to generate global daily and 8-day surface reflectance products since 2000 (Vermote et al., 2002). The 6SV code has also been implemented for correction of Landsat TM and ETM + data (Masek et al., 2006). The approach relies on inverting the aerosol effect, using the bands centered at the shortest (blue) wavelengths where the surface reflectance is generally small and the aerosol signal strong. Consequently, the accuracy of the blue and green surface reflectance is lower than in the longer wavelengths, and these bands should be used with caution (Vermote & Kotchenova, 2008; Ju, Roy, Vermote, Masek, & Kovalskyy, 2012).

A Landsat 8 OLI land surface atmospheric correction algorithm is being prototyped using the 6SV approach refined to take advantage of the narrow OLI spectral bands, improved radiometric resolution and signal to noise, and the new OLI blue band (0.43–0.45 μm). The new blue band is particularly helpful for retrieving aerosol properties, as it has shorter wavelength than the conventional OLI, TM and ETM + blue bands. Fig. 1 shows results of preliminary tests applied to a Landsat 8 OLI scene acquired over Washington D.C. and Baltimore. The true color surface reflectance and uncorrected TOA reflectance are shown in Fig. 1a and b respectively, and illustrate the impact of the correction at visible wavelengths. Fig. 1c shows the extent of cirrus cloud depicted by the shortwave infrared band (1.36–1.39μm) sensor that was specifically added to the OLI for this purpose. This band is being evaluated as an atmospheric correction pre-filter, as aerosol properties near clouds can be very different than far from clouds (Tackett & Di Girolamo, 2009). Figs. 2 and 3 illustrate full resolution surface reflectance images extracted from Fig. 1a over Dulles Airport and Baltimore Inner Harbor, respectively. The Landsat 8 OLI 15 m panchromatic band was used to pan sharpen (Tu, Huang, Hung, & Chang, 2004) these two images. The improved OLI 12-bit radiometric resolution, particularly over water, and the high level of geographic detail provided by the OLI, are clearly apparent.

4.3. Surface albedo

The surface albedo – the proportion of solar energy that is reflected by the Earth's surface – is an essential climate variable describing the energy available to drive atmospheric, land, oceanic, and cryospheric temperature and evaporation regimes as well as vegetative evapotranspiration, photosynthesis, and carbon assimilation (Schaaf, Cihlar, Belward, Dutton, & Verstraete, 2009; Schaaf, Liu, Gao, & Strahler, 2011, chap. 24). Long-term surface albedos are required by climate, biogeochemical, hydrological, and weather forecast models at a range of spatial and temporal scales. The albedo varies as a result of solar illumination, snowfall, inundation, vegetation growth, littoral variation, and with natural and anthropogenic disturbance and land cover and land use change. Improving the spatial detail and precision of surface albedo measures using Landsat is especially important in understanding the impacts of local land cover change. Variations in surface albedo, particularly in areas of permanent and seasonal snow cover, have been shown to play a significant role in the radiative forcing of the Earth system and represent a significant contributor to ongoing changes in the terrestrial energy balance (Barnes & Roy, 2010; Flanner, Shell, Barlage, Perovich, & Tschudi, 2011; Myhre, Kvalevag, & Schaaf, 2005).

Remote sensing offers the only viable method of measuring and monitoring the global heterogeneity of albedo (GCOS, 2004; Schaaf et al., 2009). Surface albedo cannot be retrieved directly from Landsat spectral bidirectional surface reflectance because of the narrow field of view, which precludes sampling of the intrinsic reflectance anisotropy of most land surfaces. However, 30 m surface albedo can be derived using the coarser resolution (500 m) MODIS Bidirectional Reflectance Distribution Function (BRDF) product (Schaaf et al., 2002, 2011, chap. 24) to capture the generalized surface anisotropy of different surface land covers, and then coupling these with concurrent 30 m Landsat spectral bidirectional surface reflectance (Shuai, Masek, Gao, & Schaaf, 2011). This approach is being used to develop a Landsat 8 OLI surface albedo algorithm to derive spectral and broadband intrinsic albedo values (white-sky albedo and black-sky albedo). The improved OLI radiometry

and atmospheric correction will provide more reliable spectral albedo, and the greater number of OLI spectral bands will contribute to improved broadband albedo values. In addition, the new OLI blue band may improve albedo retrieval over littoral areas, to help characterize estuaries, mangroves and coral reefs.

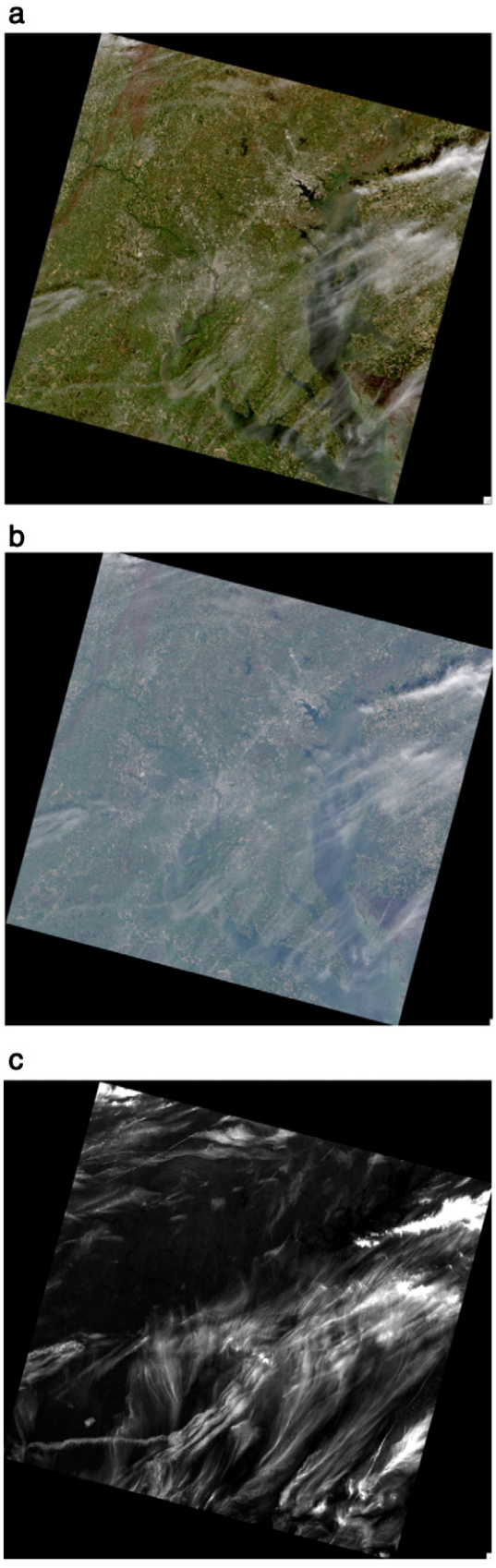

4.4. Surface temperature, evapotranspiration and drought

Land surface temperature is one of the key variables needed to describe surface states and processes critical in studies of climate, hydrology, ecology, biogeochemistry and human health (Kalma, McVicar, & McCabe, 2008; Quattrochi & Luvall, 2004). Prior to Landsat 8, the land surface temperature could not be derived reliably without use of ancillary data because of the availability of only a single Landsat thermal wavelength band. The two thermal TIRS bands are spectrally similar to two of the 1 km MODIS thermal bands and enable, for the first time, atmospheric correction of Landsat thermal imagery using split-window techniques. This will provide simpler and more accurate retrieval of surface temperature and emissivity than was possible with previous Landsat sensor data.

Landsat provides the spatial resolution and continuous record needed to capture time histories of water consumption at the scale of human use, critically, at the scale of typical agricultural fields. Landsat-based field-aggregated evapotranspiration (ET) is currently being used in a number of U.S states for water rights management (Sullivan, Huntington, & Morton, 2011) and for conjunctive management of surface and ground-water (Anderson, Allen, Morse, & Kustas, 2011; Burkhalter et al., 2013), and in other countries to estimate non-sustainable ground-water depletion (Santos, Lorite, Allen, & Tasumi, 2012). Water budgets, groundwater modeling, and expert evidence submitted for water rights hearings have relied on Landsat to identify areas and quantities of groundwater discharge consumed by natural vegetation and to define the perennial water yield (Allen, Tasumi, Morse, et al., 2007; Burns & Drici, 2011; NSEO, 2012). Many groundwater discharge areas are small or narrow and have high spatial variability, requiring Landsat's spatial resolution to estimate spatially representative and accurate ET fluxes. Fig. 4 shows a map of ET produced from Landsat 8 for a coastal area of California about 150 km south of where Landsat 8 was launched. The center image is relative ET produced by the METRIC surface energy balance application (Allen, Tasumi, & Trezza, 2007), expressed as a fraction of maximum, weather-based reference ET (ETrF) for the day, shown at the native 100 m TIRS resolution. The right image is relative ET produced by METRIC following a 'sharpening' of the thermal data to the 30 m OLI resolution, achieved by associating variations in surface temperature and shortwave OLI vegetation indices (Trezza et al., 2008). Outlines of areas of water consumption associated with individual fields become clearer after thermal sharpening, and the consistency of ET between field edges and field centers supports the usefulness of the sharpening to better define total water consumption associated with individual fields and water rights.

Continental-scale thermal-based ETrF anomaly maps generated using coarse-scale geostationary satellite thermal data have been shown to provide a robust and high-resolution alternative to precipitation-based indices for drought monitoring (Anderson, Hain, Wardlow, Mecikalski, & Kustas, 2011; Anderson et al., 2013). Landsat scale ET time-series provide a unique opportunity to investigate field-scale vegetation stress and to study how drought vulnerability varies spatially with plant-functional type, land/water management and edaphic condition, and to enhance drought early warning systems for targeted mitigation efforts and improved yield estimation (Anderson, Kustas, et al., 2011). Fusion of ET data-streams from Landsat and daily MODIS data provide the

Fig. 1. a. Prototype Landsat 8 OLI surface reflectance product derived from a 185 km × 180 km L1T image acquired over Chesapeake Bay, MD, USA, April 21 2013. True-color composite of the OLI red (0.630–0.680 μm), green (0.525–0.600 μm) and blue (0.450–0.515 μm) bands. b. Top of atmosphere true-color composite for the same scene and OLI bands shown in Fig. 1a. Illustrated using the same contrast stretch as for Fig. 1a. c. Cirrus, and also other clouds, apparent in the new OLI cirrus band (1.360–1.390 μm) for the scene shown in Fig. 1a and b.

Fig. 2. Full resolution depiction of Dulles Airport, in Virginia just west of Washington, DC, extracted from the OLI surface reflectance image (Fig. 1a). The OLI panchromatic band (0.500–0.680 μm) has been used to sharpen the resolution of the red, green and blue bands. A region of 9 km × 9 km is shown.

opportunity to enable more timely detection of incipient crop stress (Cammalleri, Anderson, Gao, Hain, & Kustas, 2013). Landsat 8 will continue to serve as the primary data source for the development of technologies for estimating cumulative water consumption over growing-season timescales, for estimating groundwater discharge, perennial water yield, and for monitoring changes in water use and availability as populations increase and pressures to develop new freshwater resources rise.

4.5. Agriculture

Landsat-based agricultural applications were developed shortly after the launch of Landsat 1 and have been subject to multi-agency funded support through initiatives including the Large Area Crop Inventory Experiment (LACIE) (MacDonald, Hall, & Erb, 1976) and the Agriculture and Resources Inventory Surveys through Aerospace Remote Sensing (AgRISTARS) Program (AgRISTARS Program Support Staff, 1981). Landsat 8 will build upon this rich history, adding to the temporal archive of agricultural change information and allowing for continued monitoring.

The U.S. Department of Agricultural (USDA) uses Landsat and Landsat-like satellite data to monitor cropping systems domestically and abroad. A flagship example is the Cropland Data Layer (CDL) which is annually generated to define over 100 land cover and crop type classes at 30 m for all the conterminous U.S. It is used primarily to help estimate crop area of dominant commodities and supplements information from ongoing ground-based surveys (USDA, 2013). The CDL is generated using a supervised classification approach with extensive agricultural ground truth (Boryan, Yang, Mueller, & Craig, 2011; Johnson & Mueller, 2010) applied to a variety of sensor data including from Landsat 5 TM, Landsat 7 ETM+, Indian Remote Sensing Resourcesat-1 Advanced Wide Field Sensor (AWiFS), and Disaster Monitoring Constellation (DMC) Demios-1 and UK-2 (Johnson, 2008). Non-U.S. satellite data have been utilized to complement Landsat data because they have a more frequent revisit rate (less than 16 days) and do not suffer from the Landsat 7 ETM+ scan line corrector problem (Markham et al., 2004). The USDA has already begun integrating Landsat 8 data into the CDL generation to benefit from the greater data coverage and the improved OLI radiometric resolution and spectral band locations. Fig. 5 shows CDL for 2012 and 2013 made with DMC and with Landsat 8 OLI data respectively. It is anticipated that because of the improved radiometric resolution and spectral characteristics combined with the greater number of images collected, Landsat 8 will be a key data source for USDA programs and reduce organizational reliance on non-US satellite assets that have incremental costs and processing requirements.

Satellite-based crop yield estimation is also of interest to the USDA and others because in situ surveys are expensive and often do not capture rapid within season changes. Furthermore, in many regions

Fig. 3. Full resolution depiction of Baltimore, Maryland, Inner Harbor extracted from the OLI surface reflectance image (Fig. 1a). The OLI panchromatic band (0.500–0.680 μm) has been used to sharpen the resolution of the red, green and blue bands. A region of 9 km × 9 km is shown.

there are no reliable crop condition statistics (Becker-Reshef et al., 2010), which is of concern because crop supply uncertainty often increases commodity price volatility (Food & Agriculture Organization, FAO of the United Nations, 2011). To date, coarse spatial resolution satellite data have been used predominantly, and satellite-derived yield products remain in the research domain (Bolton & Friedl, 2013; Doraiswamy et al., 2005). Landsat provides the appropriate field scale spatial resolution and continuous record needed to capture crop growth in many regions of the world (Doraiswamy et al., 2004; Gitelson et al., 2012; Lobell, Ortiz-Monasterio, Asner, Naylor, & Falcon, 2005), particularly in regions with smaller field sizes or mosaic plantings. However, the 16-day Landsat revisit combined with cloud cover can limit the reliable documentation of phenology compared to coarse resolution near daily coverage polar orbiting systems such as MODIS (Kovalskyy, Roy, Zhang, & Ju, 2011), which is critical for monitoring growing season crop productivity.

Field-level, and within-field, monitoring is important for the early detection of plant disease and weed infestation, to assess the efficacy of agricultural management practices, and to monitor the impacts of ephemeral meteorological events. Although conventionally undertaken with airborne and high resolution satellite data, the improved geometric and radiometric fidelity of Landsat 8 OLI data are expected to provide new opportunities in this domain. Certainly the water consumption associated with individual fields (Fig. 4) and the use of pan sharpening with the 15 m panchromatic band (Figs. 2 and 3) indicate potential for within field monitoring, particularly in large scale mechanized agricultural areas.

Landsat 8 data are now part of the satellite data collections used by the USDA, and are likely to be used by other international governmental agencies, agribusiness, and individual agricultural producers. Integration with Landsat 7, alongside other sensors, such as AWiFS, DMC and Sentinel-2, will allow for the generation of denser temporal profiles of croplands to enhance agricultural monitoring efforts. However, the biggest improvement from Landsat 8 will most likely come from the improved global collection capacity, allowing improved ability to map global agricultural regions consistently and in greater detail.

4.6. Land cover, condition, disturbance and change

Landsat data have been used since the beginning of the Landsat program to monitor the status and changes of the Earth's land cover and condition and have become the core of many institutional large-area land cover mapping and monitoring initiatives. Additionally, the combination of free Landsat data and the increasing affordability of computer

Fig. 4. A 11 km × 22 km coastal area near Ventura, California from a Landsat 8 L1T image acquired May 4 2013. Left: false color image of OLI short-wave infrared (1.57–1.65 μm), near-infrared (0.85–0.88 μm) and red (0.64–0.67 μm) expressed as red, green, blue, Center: relative ET produced by METRIC surface energy balance application using native resolution 100 m TIRS thermal bands, Right: relative ET produced by METRIC following 'sharpening' of the TIRS thermal data.

processing and storage hardware have catalyzed a blossoming of novel research in both mapping and change detection. Landsat 8 continuity extends the record that is the foundation for land change investigations, and preserves the institutional investments made by land change science and applications programs.

4.6.1. Systematic institutional large-area land cover mapping and monitoring initiatives

US Federal agencies have relied on Landsat data for operational land cover mapping since the 1990's. The United States Multi-Resolution Land Characteristics (MRLC) Consortium was initiated during the Landsat commercial in 1994 to cost-share the compilation of a national dataset of processed Landsat scenes for use in various agency land cover projects. The USGS National Land Cover Dataset (Fry et al., 2011), the USGS Gap Analysis Project natural vegetation mapping project (Jennings, 2000), and the NOAA Coastal Change Analysis Program (C-CAP) coastal zone land cover mapping (Dobson et al., 1995) were the initial products of the joint data buy. These initiatives continue, and now include the Landscape Fire and Resource Management Planning Tools Project (LANDFIRE) (Rollins, 2009; Vogelmann et al., 2011) and the USDA Cropland Data Layer (see Section 4.5). Other countries have adopted Landsat for national mapping activities. Canada used circa 2000 Landsat TM and ETM+ data to produce the Earth Observation for Sustainable Development map of forests (EOSD) (Wulder et al., 2008) and this detailed product plays a role in a variety of Canadian applications including the National Forest Inventory, forest fragmentation assessment (Soverel, Coops, White, & Wulder, 2010), and conservation protection (Andrew, Wulder, & Coops, 2012; Cardille, White, Wulder, & Holland, 2012). The Australian Landsat archive currently underpins natural resource management at state levels (Armston, Denham, Danaher, Scarth, & Moffiet, 2009) and supports national scale carbon inventories (Lehmann, Wallace, Caccetta, Furby, & Zdunic, 2013) using Geoscience Australia surface reflectance Landsat 5 and Landsat 7 data (Li et al., 2010).

Landsat data anchor international tropical forest monitoring efforts. NASA's Landsat Pathfinder Program laid the foundation for large-area Landsat mapping of tropical regions (Justice et al., 1995; Skole & Tucker, 1993). The operational PRODES Project (Projeto de Monitoramento do Desflorestamento na Amazonia Legal), conducted by Brazil's National Institute for Space Research (INPE), has been using Landsat data to monitor deforestation rates across the Brazilian Amazon annually since 1988 (INPE, 2013; Shimabukuro, Batista, Mello, Moreira, & Duarte, 1998). The Observatoire Satellital des Forêts d'Afrique Centrale (OSFAC) initiative is using Landsat and other data to monitor Congo Basin forests (Hansen et al., 2008). The European Commission's Joint Research Centre TREES-III project uses a pan-tropical grid sampling approach to characterize tropical forest loss for 20 by 20 km sample blocks of Landsat TM data from 2000 to 2010 (Achard et al., 2002; Beuchle et al., 2011; Mayaux et al., 2013). Hansen et al. (2013) recently documented a decade of global forest gains and losses using Landsat ETM+ data. As a result of the success of these and other tropical forest monitoring investigations, Landsat data are a key input to the UN-REDD (Reducing Emissions from Deforestation and forest Degradation) Programme that was launched in 2008 to support the measurement, reporting and verification of forest cover and carbon stocks in developing countries (GOFC-GOLD, 2012).

Landsat 8 data will enable these initiatives to continue, thereby ensuring relevance to their resource management, policy, research and application user communities. In particular, the continuity of the information content of the Landsat TM and ETM+ reflective wavelength bands, including the short-wave infrared bands to improve discrimination of bare soil from non-photosynthetic vegetation (Ustin, Roberts, Gamon, Asner, & Green, 2004) and to distinguish broadleaf and evergreen forest types (Horler & Ahern, 1986), is critical. In a classification

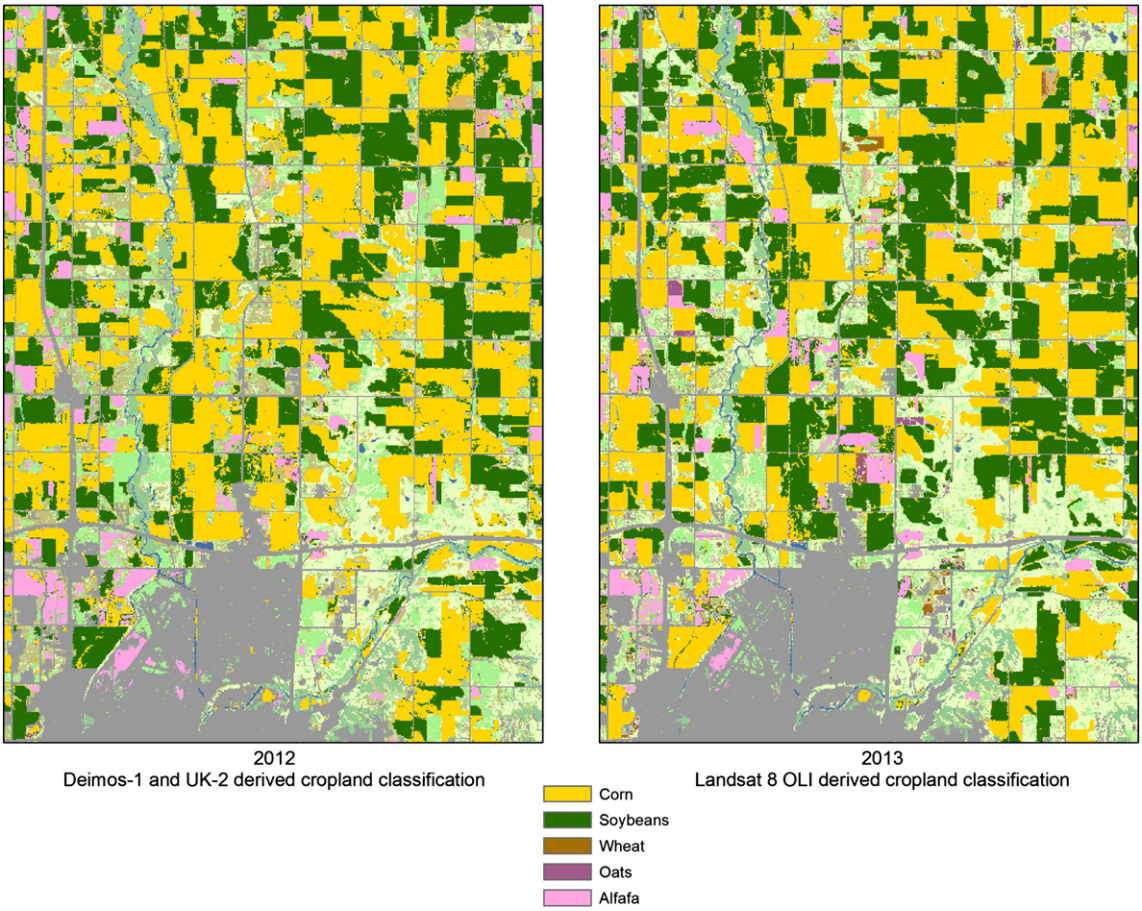

Fig. 5. Summer 2012 (left) and 2013 (right) USDA/NASS Cropland Data Layer (CDL) for a 17 km × 24 km portion of southeastern South Dakota. The 2012 CDL was derived by supervised classification of the red, green and near infrared wavelength 22 m Deimos-1 and UK-2 data. The 2013 CDL was derived by supervised classification of the 30 m Landsat 8 OLI reflective wavelength bands. The northern part of the city of Sioux Falls is shown as gray and is located in the south of the image. The USGS Earth Resources Observation and Science (EROS) center, home of the U.S. Landsat archive, is located in the northeast image corner.

context, the improved OLI signal-to-noise ratio promises to enable better discrimination of low reflectance targets, and to improve discrimination among various soil and non-photosynthetic vegetation targets. The new shortwave infrared band will improve detection of cirrus clouds (Fig. 1c) and facilitate more reliable land cover mapping. This is particularly important in persistently cloudy areas, where less reliable cloud detection has necessitated aggressive cloud masking and reliance on temporal compositing of Landsat data from very different time periods (Lindquist, Hansen, Roy, & Justice, 2008). International studies, particularly in the tropics and high latitudes, will also benefit from the increased daily image acquisition capacity and improved image geodetic properties, the latter should enable more accurate image geometry in cloudy regions. In addition, the Landsat 8 OLI panchromatic band has a narrower bandpass compared to previous Landsat sensors to provide greater contrast between vegetated and bare surfaces, and will enhance classification training and validation data collection.

4.6.2. Emerging mapping and change detection approaches

Although spatial and spectral properties have made Landsat data the workhorse of land surface characterization, the opening of the Landsat archive has fostered new analytical time series approaches for describing land surface condition and dynamics. The critical change has been a movement from image-based to pixel-based analysis. Because Landsat data are now free and readily available, users are able to develop approaches based upon using all the available Landsat images for a given region and time period rather than just a select subset of cloud-free images. This has led to the development of new time-series change characterization approaches and new cloud and shadow masking, mosaicking, and temporal compositing approaches, whereby the highest quality pixels from multiple acquisitions are utilized. For example, temporal compositing approaches are now being used to select a best Landsat observation from all the Landsat observations collected over some reporting period to generate gridded weekly, monthly, seasonal and annual composites (Roy et al., 2010) that have been used to map conterminous U.S. 30 m percent tree cover, bare ground, and five year tree cover loss and bare ground gain (Hansen et al., 2011; 2014). Recent Landsat mapping and change detection approaches have focused on quantifying land cover change over an unprecedented range of time scales (Cohen, Zhiqiang, & Kennedy, 2010) and using novel time series approaches (Zhu, Woodcock, & Olofsson, 2012; Brooks et al., 2013). For example, the Vegetation Change Tracker (VCT) provides a set of automated algorithms designed to detect forest disturbance using Landsat time-series (Huang et al., 2010) and has been used to estimate annual forest disturbance rates for the conterminous U.S. (Masek et al., 2013). The LandTrendr algorithms capture abrupt disturbance events in forests (Kennedy, Yang, & Cohen, 2010) and other land cover changes, allowing linkage of disturbance rates with changes in policy and economic conditions (Griffiths et al., 2012; Kennedy et al., 2012). All pixel-level disturbance and change mapping approaches will benefit from the improved quality and data coverage of Landsat 8. Landsat 8 data represent an extension of the unbroken Landsat spectral record, providing a set of relatively consistent spectral bands critical for capturing many land cover processes and providing a baseline for temporal comparison.

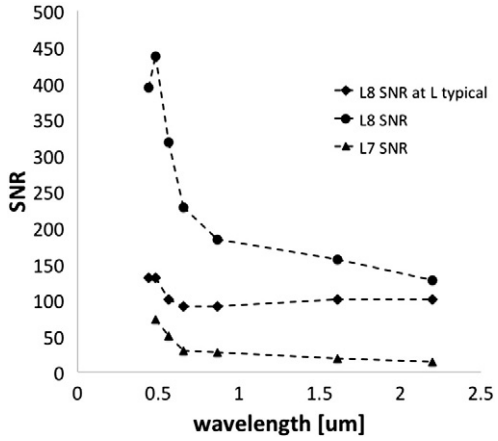

Fig. 6. Signal-to-Noise Ratio (SNR) for uniform water regions extracted over a region of uniform brightness in the Red Sea from Landsat 8 OLI (circles) and Landsat 7 ETM + (triangles), along with the specified SNR for Landsat 8 at typical radiance (L) levels (diamonds).

4.7. Fresh and coastal water

Surface fresh water sources comprise a small fraction of the global water pool, yet they are the foundation of life in terrestrial ecosystems. Present knowledge on fresh water distributions is limited at regional and global scales. Global databases of lakes, reservoirs and wetlands exist, but they have not been generated in a systematic manner or using the same data sources (Lehner & Döll, 2004). The Shuttle Radar Topography Mission (SRTM) Water Body Dataset (SWBD) was developed to improve the quality of SRTM digital elevation products (SWBD, 2005), and was subsequently improved by the global 250 m MODIS water mask product (Carroll, Townshend, Dimiceli, Noojipady, & Sohlberg, 2009). The 15 m and 30 m resolution of the Landsat 8 OLI, combined with high global data availability, present a unique opportunity to provide the first and most up-to-date global inventory of the world's lakes at high spatial resolution and positional accuracy using recent Landsat algorithms (Li & Sheng, 2012; Sheng & Li, 2011; Smith, Sheng, MacDonald, & Hinzman, 2005). This global high-resolution lake database is expected to contain millions of lakes with a size of one hectare or larger (Downing et al., 2006; Meybeck, 1995).

In addition to measuring the extent of water bodies satellite data have utility for water quality information retrieval. The Landsat TM and ETM + sensors have limited capability to map water quality in fresh and coastal waters and have been largely restricted to mapping turbidity or single constituent variations (assuming all observed change was due to only one constituent). (Olmanson, Bauer, & Brezonik, 2008; Onderka & Pekárová, 2008). These limitations are due to the relatively low signal-to-noise ratio (SNR) of previous Landsat sensors as well as to the limited number of spectral bands in the visible region where water quality spectral signatures are manifest.

Fig. 3 illustrates the quality of OLI data over the Baltimore Inner Harbor, using the heritage Landsat visible bands, illustrating qualitatively the improved radiometric fidelity of these data over water. The SNR possible with OLI and the actual performance on orbit have considerably exceeded expectations. This is illustrated in Fig. 6, comparing Landsat 8 OLI SNR values for a uniform sample of water in the Red Sea with a similar sample taken from a Landsat 7 ETM + image and the instrument

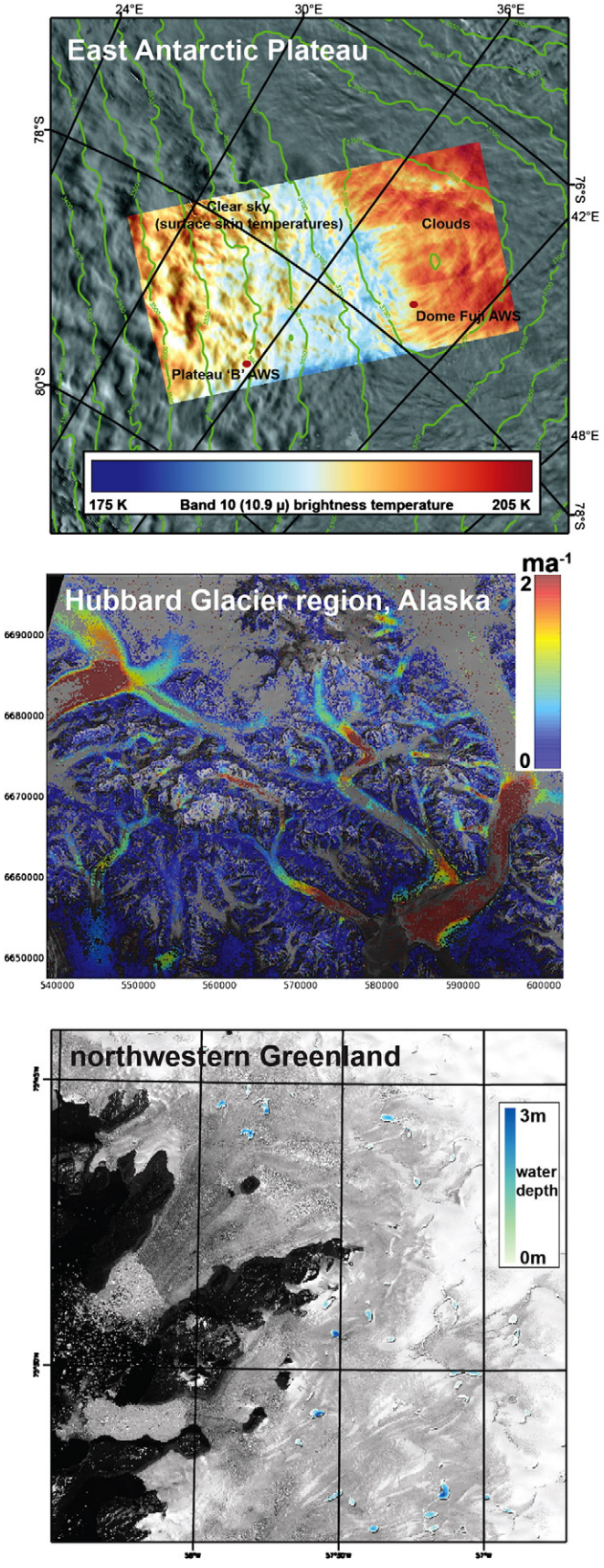

Fig. 7. Preliminary Landsat 8 cryospheric applications. Top: winter thermal TIRS 10.6–11.2 m brightness temperatures (BT) over the East Antarctic Plateau near Dome F acquired on 31 July 2013, showing low BT in clear-sky areas south of the dome summit (elevation contours in green) and nearby Automatic Weather Stations (AWS), Middle: glacier ice speed of a region of southeastern Alaska derived by surface feature tracking from a pair of Landsat-8 OLI images acquired 12 July and 13 August 2013 (color bar at right is in meters/day), Bottom: meltwater lake depth map for a small region of northwest Greenland from Landsat 8 OLI image acquired 18 July 2013.

specified values at a typical radiance level. These high SNR values are extremely important for water constituent mapping because the very low signal from water causes variations in water quality to be lost in the noise of low SNR systems (Gordon & Clark, 1981).

Atmospheric correction over coastal waters is particularly challenging because of the much lower SNR compared to land; consequently, water-specific Landsat 8 atmospheric correction techniques are being developed that take advantage of the new shorter wavelength blue band (Gerace & Schott, 2012). Using simulated data and spectral matching algorithms, Gerace, Schott, and Nevins (2013) demonstrated that the combination of the new OLI blue band and the improved SNR should reduce error in constituent retrieval values to about half of the error expected from Landsat 7 ETM+, with most of this improvement attributable to the improved SNR. These results were for the simultaneous retrieval of chlorophyll, colored dissolved organic material (CDOM) and suspended material (SM) at the instrument specified SNR. Given the SNR values observed on orbit (Fig. 6), the expected errors should be again reduced by one half (total reduction to about one fourth the ETM+ expected errors). As a result of these simulated studies and the initial observed OLI SNR values on orbit, we expect Landsat 8 to enable a new era of water quality monitoring in the critical coastal and fresh water regions of the globe.

4.8. Snow and ice

Landsat cryospheric applications began with the earliest Landsat missions, in particular with the extensive 1972–1975 Antarctic coverage by Landsat 1, 2, and 3 (Swithinbank, 1988). Landsat data have remained a central tool for documenting the profound changes throughout the global cryosphere in the past 40 years (e.g., Bindschadler, Dowdeswell, Hall, & Winther, 2001; Bindschadler et al., 2008; Williams, Ferrigno, Swithinbank, Lucchitta, & Seekins, 1995). Cryospheric research will benefit from the improved geometric and radiometric fidelity of the Landsat 8 OLI visible bands, allowing subtle surface features of the large ice sheets to be better mapped and tracked for flow velocity (Bindschadler, 2003). High radiometric sensitivity in the TIRS bands also holds promise for better mapping of summertime ocean surface temperature in fjords adjacent to tidewater and floating-front glaciers, providing insight into ice-ocean interactions that can dramatically affect ice front retreat and flow speed (Mankoff, Jacobs, Tulaczyk, & Stammerjohn, 2012; Motyka, Hunter, Echelmeyer, & Connor, 2003). The TIRS data also have potential for mapping debris-cover thickness over mountain glaciers through seasonal and diurnal variations in temperature as thin debris cover shows a modified response to solar heating due to the underlying ice (Bhambri, Bolch, & Chaujar, 2011; Shukla, Arora, & Gupta, 2010).

Chief among the specific cryospheric issues that will be addressed with Landsat-8 data is the determination of the net ice outflow of the great ice sheets, including variation over time, and mapping the ice flow velocity of the world's mountain glaciers. This is currently conducted by automated feature tracking in sequential time series images (Berthier et al., 2005; Debella-Gilo & Kääb, 2011; Scambos, Dutkiewitcz, Wilson, & Bindschadler, 1992). The increased global OLI data acquisition will lead to more frequent cloud-free image pairs suitable for flow mapping, and the improved OLI data geometry and radiometry should improve tracking accuracy and the ability to track ice flow in low-contrast areas of glaciers and ice sheets (Bindschadler, 2003).

Examples of ongoing Landsat 8 applications to polar and glacier ice study areas demonstrate several useful techniques using the OLI and TIRS data (Fig. 7). In Fig. 7 (top), a very low temperature calibration test site in the high-elevation areas of East Antarctica is illustrated. Increased thermal sensor precision and extended calibrated temperature range at the 100 m TIRS resolution can be used to investigate the spatial distribution of extremely low ice sheet temperatures. In Fig. 7 (middle) the geolocation and high radiometric precision of the OLI panchromatic band facilitate ice velocity mapping using image cross-correlation algorithms based on refinements to established algorithms. Landsat 8 will also contribute to detailed mapping of surface melt ponds occurring on glaciers and ice sheets, including their extent, depth, and volume, with enhanced precision due to the higher radiometry relative to past Landsat studies (e.g., Tedesco & Steiner, 2011). Empirical relationships between field-based estimates of lake-bottom albedo and the decline in radiance in the OLI green (0.525–0.600 μm) reflectance with water depth can be used to define meltwater depth (Fig. 7, bottom). This capability is particularly notable as surface water on ice sheets and glaciers is difficult to monitor but can have a complex interaction with the underlying ice, through fracture, penetration, and sub-glacial lubrication (Das et al., 2008; Scambos, Bohlander, Shuman, & Skvarca, 2004; Stearns, Smith, & Hamilton, 2008; Zwally et al., 2002).

5. Higher-Level Landsat product generation needs, opportunities and challenges

The provision of 'higher-level' Landsat products, i.e., geographically seamless, gridded products that have been subject to geophysical transformations and processed to derive environmental variables over different time periods (monthly, seasonal, annual), have been advocated by the LST and by the user community. Higher-level products are needed to meet demands for consistently processed, moderate spatial resolution, large area, long-term terrestrial data records for climate and global change studies, to help national and international reporting linked to multilateral environmental agreements, and for regional and national resource management applications.

The Millennium Ecosystem Assessment (Carpenter et al., 2006) and outcomes of the Rio +20 United Nations Conference on Sustainable Development (UN, 2012) highlighted the need for transparent, systematic, and repeatable measures of a variety of ecosystem characteristics. The concept of a climate data record has been introduced as a data set designed to enable study of long-term climate change, with 'long-term' meaning year-to-year and decade-to-decade change, (NRC, 2000). The 40+ year continuity of the Landsat program, with consecutive, temporally overlapping Landsat observatories and cross-sensor calibration, is a key reason the Landsat program has value for climate studies (Trenberth et al., 2013). The Global Climate Observing System has identified a set of Essential Climate Variables (ECVs) needed in support of the United Nations Framework Convention on Climate Change (GCOS-154, 2011), and listed the following terrestrial ECVs as feasible for sustained monitoring from satellite data: snow areal extent; outlines of glaciers and ice caps; ice sheet elevation changes; lake level and area; surface reflectance anisotropy and black and white sky albedo; land cover type and maps for detection of land cover change; fraction of absorbed photosynthetically active radiation (FAPAR); leaf area index (LAI); above-ground forest biomass; burned area and active fire detection; soil moisture; and land surface temperature. The preliminary LST evaluation of Landsat 8 capabilities and identification of new science and applications described in Section 4 illustrate that the majority of these ECVs can be retrieved directly or indirectly from Landsat data. Of the ECVs identified, only ice sheet elevation changes, soil moisture, and above-ground forest biomass cannot be reliably retrieved from Landsat 8 or predecessor Landsat sensor data. However, Landsat-based forest biomass estimates can be made in certain biomes, such as boreal forests, with accuracies comparable to estimates derived using higher spatial resolution satellite and airborne data (Mora, Wulder, White, & Hobart, 2013). The fAPAR and LAI can be derived by empirical biome or land cover class specific parameterization of NDVI (Butson & Fernandes, 2004) or by model inversion against Landsat reflectance (Ganguly et al., 2012). Landsat burned area mapping involves a high degree of human intervention (Bastarrika, Chuvieco, & Martin, 2011) and large area Landsat burned area mapping initiatives have significant reporting lags (Eidenshink et al., 2007). Landsat active fire detection algorithms have also been developed but have limited sampling capabilities (Schroeder et al., 2008).

The experience of generating and distributing global decadal scale coarse spatial resolution land products derived from MODIS and Advanced Very High Resolution Radiometer (AVHRR) data (Justice et al., 1998; Tucker et al., 2005) is informative of the opportunities and challenges to generating higher-level Landsat products. Global long-term AVHRR land surface data records have been derived to advance understanding of the terrestrial carbon and biogeochemical cycles and interactions with climate (Myneni, Tucker, Asrar, & Keeling, 1998). To

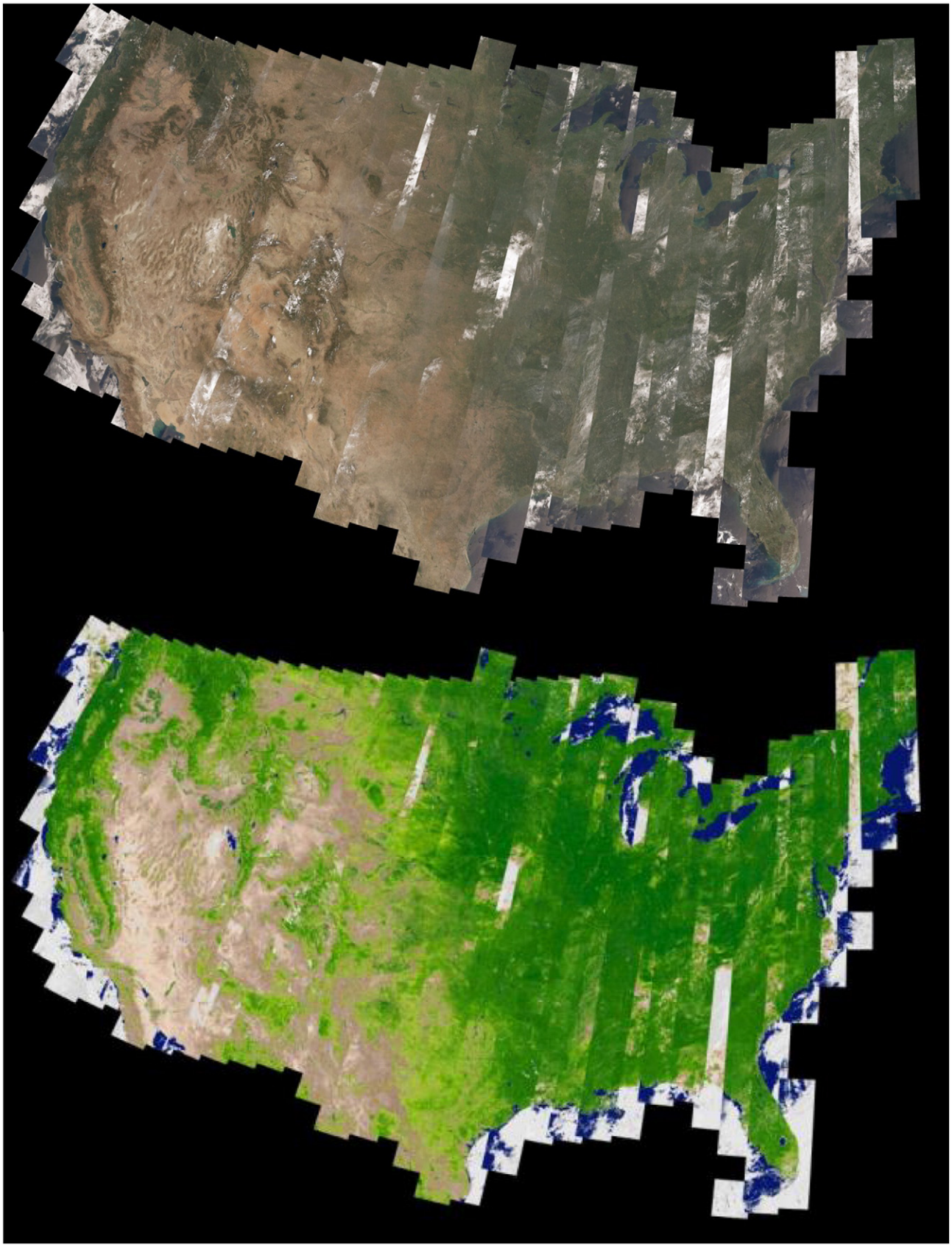

date, however, no definitively processed long-term AVHRR land data record has been generated and those that are publically available are subject to scientific debate (Beck et al., 2011). This is because, unlike Landsat, the AVHRR sensors have no onboard reflective wavelength calibration capability and they were not designed for land surface monitoring (Vermote, Saleous, & Holben, 1995; Wu, Sullivan, & Heidinger, 2010). MODIS combines characteristics of the AVHRR and Landsat sensor designs and includes onboard reflective and thermal wavelength calibration systems (Justice et al., 1998). A suite of higher-level MODIS land products are being generated to meet the needs of the global change research community, with the recognition that the products are also used at regional scales and in support of applications (Justice et al., 2002; Masuoka et al., 2011, chap. 22). The acceptance and utility of the MODIS Land products by the resource management, policy, research and application communities indicate the need for similar products and product generation approaches but at Landsat resolution.

It is feasible to process long-term and large-area Landsat data sets to provide a medium spatial resolution analog to the coarse spatial resolution higher-level land products generated from the MODIS and AVHRR data streams. The Web-enabled Landsat Data (WELD) project has started to demonstrate this capability by generating ten years of 30 m weekly, seasonal, monthly and annual composited Landsat 7 ETM+ mosaics of the conterminous United States (CONUS) and Alaska (Roy et al., 2010). The WELD products enable the development of turnkey approaches to, for example, land cover and land cover change characterization (Hansen et al., 2011; 2014), by employing systematic and automated Landsat processing, including conversion of digital numbers to calibrated top of atmosphere reflectance and brightness temperature, cloud masking, and reprojection into a gridded continental map projection. The WELD processing has been adapted and applied to Landsat 8 data. Fig. 8 shows the WELD processing applied to all the Landsat 8 L1T data acquired over the CONUS in August 2013. Unlike currently available WELD Landsat 7 ETM+ products (WELD, 2013), the reflectance saturation usually seen over clouds is not evident due to the improved OLI dynamic range, there are no missing data because the improved Landsat 8 geolocation enables more images to be processed to L1T products, and there are no missing data due to the ETM+ SLC-off issue.

Additional steps are needed during the Landsat 8 era if the needs of the global change research user community are to be met. Not least is the need to generate global coverage Landsat higher-level products for the entire Landsat sensor data record. These data should be atmospherically corrected to provide an accurate and stable surface reflectance record. Algorithms to combine contemporaneous Landsat sensor data, e.g. Landsat 5 and 7, or Landsat 7 and 8, should also be developed to provide more frequent acquisition coverage and improved probabilities of acquiring cloud-free land observations (Kovalskyy & Roy, 2013). Higher-level product generation algorithms that are computationally efficient and automated should be developed as approaches that require high levels of user intervention will not be scalable. The global annual Landsat data volume is more than an order of magnitude greater than for MODIS, requiring processing on high performance supercomputers with petabyte data storage solutions (Nemani, Votava, Michaelis, Melton, & Milesi, 2011). Distribution will also need to be scaled appropriately. Recent developments in web services and value added web product delivery systems have the potential to provide natural resource managers, policy makers and researchers with an unprecedented capacity to access, analyze and interpret higher-level products derived from the multi-petabyte scale archive of global Landsat data. In the next decade, the ability to extract Landsat 1–8 time series of derived environmental information at any pixel location globally is desired. Moreover, there are significant, but currently unrealized, opportunities for fast and automated processing to systematically produce near-real time Landsat 8 higher-level monitoring products, for example, to generate ET and drought information (Section 4.4) or disturbance information (Section 4.6).

6. International synergies between Landsat and other moderate resolution optical wavelength remote sensing satellites

The value of Landsat data and products is well established. A main shortcoming, clearly articulated in the above sections, remains the need for more frequent observations to mitigate atmospheric effects and to monitor high temporal frequency phenomena. More frequent observations provide (a) more opportunities for cloud-free, shadow-free, and atmospherically uncontaminated surface observations without missing data, within desired annual, seasonal and monthly windows, (b) increasingly detailed descriptions of time-dependent phenomena, and (c) more reliable time-series and change detection analyses. Improving the Landsat temporal resolution can be achieved by launching more Landsat sensors, to provide a constellation, increasing the imaging swath width, or by combining Landsat data with data from other comparable remote sensing satellites.

There are a number of satellites with spatial and spectral characteristics similar to those of Landsat (Stoney, 2008): at least 20 missions carrying moderate spatial resolution multispectral imagers were operational as of 30th June 2013 (Belward & Skoien, under review). In particular, Europe's Copernicus Earth Observation program includes two planned Sentinel-2 satellites designed to provide, under a free and open data policy, multiple global acquisitions with similar spectral and spatial characteristics as Landsat. The Multi Spectral Instrument (MSI) onboard Sentinel-2 has 13 spectral bands ranging from 0.433 μm to 2.19 μm; four 10 m visible and near-infrared bands, six 20 m red edge, near-infrared and SWIR bands, and three 60 m bands for characterizing aerosols, water vapor and cirrus clouds (Drusch et al., 2012). Landsat 8 and Sentinel-2 pre-launch cross-calibration was undertaken (Section 4.1) to specifically support their combined data use. Scientific and applications uses are maximized through known and communicated calibration characteristics. Landsat is currently the only satellite program to provide consistent, cross-calibrated data spanning more than four decades (Chander, Markham, & Helder, 2009; Markham & Helder, 2012), which gives the program a crucial role in the provision of terrestrial essential climate variables and long-term climate data records. The addition of other sensors and space agencies to implement instrument cross-calibration will be of considerable benefit to the user community. Complementary to calibration activities is a recommendation to move towards increasingly standardized processing, empowering users to integrate data from different systems into science and applications in a seamless fashion. A central question concerns how data from additional sensors can be integrated in a systematic and robust fashion to advance global land monitoring capabilities, with options reviewed in Wulder et al. (2011).

At the international level, the needs for and utility of information provided by satellites is clear: government and/or private entities in 32 sovereign states/geopolitical blocs have financed at least 186 land cover observing missions over the last four decades (Belward & Skoien, under review; Stoney, 2008). Since the 1970s the average number of land imaging satellites launched per-year has increased from two to over nine, average longevity has increased almost threefold, and costs of 'entry-level' systems is falling. Free and open data access stimulates new science and

Fig. 8. Conterminous United States Landsat 8 monthly WELD product browse images, August 2013, equal area Albers projection. Generated from all the available (890) August 2013 OLI scenes processed to L1T. Browse images composed of 16,500 × 11,000 300 m pixels each generated from 10 × 10 30 m OLI pixels. Top: Top of atmosphere (TOA) true color reflectance shown with a similar stretch as Fig. 1b. Bottom: TOA Normalized Difference Vegetation Index (NDVI) displayed with the standard MODIS NDVI color palette provided by the University of Arizona Vegetation Index and Phenology Laboratory.

applications, but alternative business models and lower costs stimulate wider system ownership. For example, the data sharing and common ground segment established by the Disaster Monitoring Constellation (DMC) have enabled launches of land imaging systems by agencies in Europe, Africa and Asia (Da Silva Curiel et al., 2005). Whilst more people in more countries have access to global land surface observations from space than ever before, a note of caution is needed. Smaller and lighter satellites may be cheaper to build and launch (Xue, Li, Guang, Zhang, & Guo, 2008), but there is an inescapable need for tightly specified, high reliability, high performance systems such as Landsat to maintain long–term consistent data records and facilitate fusion of data from different satellites. Satellite costs rise as performance specifications and reliability rise. The use of proven technologies, for example through follow-on missions of similar sensors, such as the two Sentinel-2 sensors, or the two MODIS sensors onboard the Terra and Aqua satellites, is one means to control costs and shorten development timelines. In all cases, restrictive data policies and data access limitations should be avoided. Explorative cross-platform experiments of benefit to the wider research community are required, and realistically only made possible by the free and open access to analysis ready data products.

7. Conclusion

The successful launch of Landsat 8 is planned to extend the 40-year Landsat record at least another 5 years, further advancing global change research, while protecting and maximizing the previous investments in Landsat. The importance of continuity of the Landsat record cannot be underestimated. Just as the Mauna Loa, Hawaii, atmospheric CO_2 record is now considered a vital indicator of human activity, but whose continuity was also not always guaranteed (Keeling, 1998), Landsat provides the longest consistent satellite terrestrial record. The free availability of all Landsat data in the U.S. archive provides an unprecedented opportunity for analysis of the past and future terrestrial change. Terrestrial changes, both gradual and sudden, may be understood in quite different ways in the context of multi-decadal rather than decadal time series. When considering the new observations from Landsat 8 as a continuation of the complementary and calibrated previously collected Landsat series, the importance, and value, of Landsat 8 is evident.

From this communication it should be clear that Landsat 8 is an exciting collection of spatial, spectral, temporal, and radiometric (performance, accuracy, and dynamic range) resolutions, combined with robust pre- and post-launch calibration, high geometric and geodetic accuracy, as well as a systematic global acquisition strategy. Looking forward, it is critical that follow-on missions enable continuity with previous Landsat missions, including data coverage, spatial and spectral resolution, and rigorous calibration. Continuity of the information content of the Landsat TM and ETM+ reflective visible and shortwave infrared bands at 30 m is needed to monitor the surface at scales where anthropogenic change is occurring. Continuity of coincident thermal band information is required to provide cloud masking capabilities and to enable surface temperature, evapotranspiration, drought and cryospheric monitoring. Continuity of radiometric calibration is fundamental to maintain a long-term consistent Landsat data record, facilitate fusion of Landsat data with other satellite sensor data, and to enable quantitative information extraction. Based on the insights of representatives from university, government, and industry, a recent report from the US National Research Council (NRC, 2013) describes the past history of the Landsat program, the core elements of the current imaging system that require continuity, and offers some suggestions on future potential land imaging systems and observation capacities. Insights on how Landsat system costs can be reduced in the future, such as purchase of multiple spacecraft and fixed price contracting, are also described. Besides reinforcing the need and demand for Landsat data, land imaging data from Landsat increasingly appears as a necessary element of national infrastructure. In any forward looking scenario regarding Landsat, the current capacity and the benefits of continuity must be maintained, with science and applications information needs driving requirements.

This paper summarizes the Landsat Science Team (LST) efforts to establish an initial understanding of Landsat 8 capabilities and the steps ahead in support of science team identified priorities. The aims of the LST align with the current scientific and applications challenges that are known or anticipated. The thematic sections above capture what is known and how to build on that existing knowledge with the recent availability of Landsat 8 data. The sensor improvements to Landsat 8 are already showing measurement and categorization improvements, and offer refined opportunities for quantitative approaches to Landsat information extraction. These benefits arise first through improved pre-processing (e.g., atmospheric correction), and then by enabling physically-based information extraction approaches (e.g., albedo, water quality, evapotranspiration; via model inversion and data assimilation). It is also evident from the thematic sections that the continued and well understood Landsat data stream offers increased capacity for systematic production of scientifically supported higher-level Landsat products. The acceptance and utility of the MODIS land products by the resource management, policy, research and application communities indicate the need for similar products and product generation approaches with Landsat. It is important that higher-level Landsat products are community endorsed and subject to external scientific scrutiny, quality assessed, validated, and reprocessed as needed. A core challenge is to scale current capabilities to generate global coverage Landsat higher-level products for all the Landsat data record.

Landsat-like is often used to describe data from other optical wavelength remote sensing systems with a similar spatial resolution as Landsat. Detection of change and monitoring of terrestrial ecosystems using these systems is hampered by cloud cover, leading to interest in radar data (De Sy et al., 2012). The free and open access to the Landsat archive has mitigated this situation through a change from scene-based to pixel-based processing, data blending, and cross-sensor data integration. The capacity of large numbers of images to create cloud-free composites at Landsat spatial resolution has been demonstrated. Landsat 8 is offering continuity of such measures, plus an effective 8-day revisit in combination with Landsat 7. The planned launch of Sentinel-2 by the European Space Agency will offer additional unique and complementary measures. Advances made through multi-sensor data integration may provide required measurements as well as providing insights on the development and deployment of additional, lower cost, satellites to complement the well calibrated and systematically collected Landsat data series.

Landsat occupies a valuable niche in global satellite remote sensing; the platform collects images at a spatial resolution indicative of human interactions with terrestrial ecosystems yet with an image extent compatible with systematic analyses over large areas. A ground-segment based on reliable science provides free and open access to Level 1 products of known, documented, and traceable quality. The integrity of this production chain and the confidence users have in Landsat data has led to a proliferation of science and applications — the Landsat program provides an example to be emulated. By expanding the Landsat archive, and by providing improved data quality, Landsat 8 has enabled continuity and early results have shown advances in established mapping and monitoring programs, allowing for a general fostering of development of new approaches for characterizing state, condition, and dynamics of the Earth's surface. Building upon these successes, near-term emphasis should be placed on ensuring operational status for the incoming Landsat data stream and outgoing Level 1 and higher-level data products.

Acknowledgements

We are grateful to the NASA–USGS-industry Landsat Data Continuity Mission (LDCM) development team for their efforts to meet an aggressive launch schedule, and we thank the USGS Climate and Land Use Change Mission's Land Remote Sensing Program and the Earth

Resources Observation and Science (EROS) Center for co-sponsoring and funding the USGS–NASA Landsat Science Team.

References

Achard, F., Eva, H. D., Stibig, H. -J., Mayaux, P., Gallego, J., Richards, T., & Malingreau, J. -P. (2002). Determination of deforestation rates of the world's humid tropical forests. *Science*, *297*, 999–1002.

AgRISTARS Program Support Staff (1981). *AgRISTARS: Agriculture and resources inventory surveys through aerospace remote sensing, annual report—fiscal year 1980*. Houston, TX: NASA, Lyndon B. Johnson Space Center.

Allen, R. G., Tasumi, M., Morse, A., Trezza, R., Wright, J. L., Bastiaanssen, W., Kramber, W., Lorite, I. J., & Robison, C. W. (2007). Satellite-based energy balance for mapping evapotranspiration with internalized calibration (METRIC) — Applications. *Journal of Irrigation and Drainage Engineering. ASCE*, *133*, 395–406.

Allen, R. G., Tasumi, M., & Trezza, R. (2007). Satellite-based energy balance for mapping evapotranspiration with internalized calibration (METRIC) — Model. *Journal of Irrigation and Drainage Engineering. ASCE*, *133*, 380–394.

Anderson, M. C., Allen, R. G., Morse, A., & Kustas, W. P. (2011). Use of Landsat thermal imagery in monitoring evapotranspiration and managing water resources. *Remote Sensing of Environment*, *122*, 50–65.

Anderson, M. C., Hain, C. R., Otkin, J. A., Zhan, X., Mo, K. C., Svoboda, M., Wardlow, B., & Pimstein, A. (2013). An intercomparison of drought indicators based on thermal remote sensing and NLDAS-2 simulations with U.S. drought monitor classifications. *Journal of Hydrometeorology*, *14*, 1035–1056.

Anderson, M. C., Hain, C. R., Wardlow, B., Mecikalski, J. R., & Kustas, W. P. (2011). Evaluation of a drought index based on thermal remote sensing of evapotranspiration over the continental U.S. *Journal of Climate*, *24*, 2025–2044.

Anderson, M. C., Kustas, W. P., Norman, J. M., Hain, C. R., Mecikalski, J. R., Schultz, L., Gonzalez-Dugo, M. P., Cammalleri, C., d'Urso,, G., Pimstein, A., & Gao, F. (2011). Mapping daily evapotranspiration at field to continental scales using geostationary and polar orbiting satellite imagery. *Hydrology and Earth System Sciences*, *15*, 223–239.

Andrew, M. E., Wulder, M.A., & Coops, N. C. (2012). Identification of de facto protected areas in boreal Canada. *Biological Conservation*, *146*(1), 97–107.

Armston, J.D., Denham, R. J., Danaher, T. J., Scarth, P. F., & Moffiet, T. N. (2009). Prediction and validation of foliage projective cover from Landsat-5 TM and Landsat-7 ETM+ imagery. *Journal of Applied Remote Sensing*, *3*, 033540.

Arvidson, T., Gasch, J., & Goward, S. N. (2001). Landsat 7's long-term acquisition plan — an innovative approach to building a global imagery archive. *Remote Sensing of Environment*, *78*, 13–26.

Arvidson, T., Goward, S., Gasch, J., & Williams, D. (2006). Landsat-7 long-term acquisition plan: Development and validation. *Photogrammetric Engineering and Remote Sensing*, *72*, 1137–1146.

ASPRS (2006, November 6). Report to the future land imaging working group on the American Society for Photogrammetry and Remote Sensing Survey on the future of land imaging. available at. http://www.asprs.org/a/news/fli/Summary_of_Final_Results-ASPRS_Moderate_Resolution_Imagery_Survey.pdf (Last accessed October 1st 2013)

Barnes, C. A., & Roy, D. P. (2010). Radiative forcing over the conterminous United States due to contemporary land cover land use change and sensitivity to snow and interannual albedo variability. *Journal of Geophysical Research*, *115*, G04033, http://dx.doi.org/10.1029/2010JG001428.

Bastarrika, A., Chuvieco, E., & Martin, M. P. (2011). Mapping burned areas from Landsat TM/ETM plus data with a two-phase algorithm: Balancing omission and commission errors. *Remote Sensing of Environment*, *115*, 1003–1012.

Beck, H. E., McVicar, T. R., van Dijk, A. I. J. M., Schellekens, J., de Jeu, R. A.M., & Bruijnzeel, L. A. (2011). Global evaluation of four AVHRR–NDVI data sets: Inter-comparison and assessment against Landsat imagery. *Remote Sensing of Environment*, *115*, 2547–2563.

Becker-Reshef, I., Justice, C., Sullivan, M., Vermote, E., Tucker, C., Anyamba, A., Small, J., Pak, E., Masuoka, E., Schmaltz, J., Hansen, M., Pittman, K., Birkett, C., Williams, D., Reynolds, C., & Doorn, B. (2010). Monitoring global croplands with coarse resolution earth observations: The Global Agriculture Monitoring (GLAM) project. *Remote Sensing*, *2*, 1589–1609.

Belward, A. S., & Skoien, J. O. (2014). Who launched what, when and why; trends in Global Land-Cover Observation capacity from civilian Earth Observation satellites. *Photogrammetric Engineering and Remote Sensing* (under review).

Berthier, E., Vadon, H., Baratoux, D., Arnaud, Y., Vincent, C., Feigl, K. L., Rémy, F., & Legrésy, B. (2005). Surface motion of mountain glaciers derived from satellite optical imagery. *Remote Sensing of Environment*, *95*, 14–28.

Beuchle, R., Eva, H. D., Stibig, H. J., Bodart, C., Brink, A., Mayaux, P., Johansson, D., Achard, F., & Belward, A. (2011). A satellite data set for tropical forest area change assessment. *International Journal of Remote Sensing*, *32*, 7009–7031.

Bhambri, R., Bolch, T., & Chaujar, R. K. (2011). Mapping of debris-covered glaciers in the Garhwal Himalayas using ASTER DEMs and thermal data. *International Journal of Remote Sensing*, *32*, 8095–8119.

Bindschadler, R. A. (2003). Tracking sub-pixel-scale sastrugi with Advanced Land Imager. *IEEE Transactions on Geoscience and Remote Sensing*, *41*, 1373–1377.

Bindschadler, R., Dowdeswell, J., Hall, D., & Winther, J. -G. (2001). Glaciological applications with Landsat-7 imagery. Early assessments. *Remote Sensing of Environment*, *78*, 163–179.

Bindschadler, R., Vornberger, P., Fleming, A., Fox, A., Mullins, J., Binnie, D., Paulsen, S. J., Granneman, B., & Gorodetzky, D. (2008). The Landsat image mosaic of Antarctica. *Remote Sensing of Environment*, *112*, 4214–4226.

Bolton, D. K., & Friedl, M.A. (2013). Forecasting crop yield using remotely sensed vegetation indices and crop phenology metrics. *Agricultural and Forest Meteorology*, *173*, 74–84.

Boryan, C., Yang, Z., Mueller, R., & Craig, M. (2011). Monitoring US agriculture: The US Department of Agriculture, National Agricultural Statistics Service, cropland data layer program. *Geocarto International*, *26*, 341–358.

Brooks, E. B., Wynne, R. H., Thomas, V. A., Blinn, C. E., & Coulston, J. W. (2013). On-the-fly massively multitemporal change detection using statistical quality control charts and Landsat data. *IEEE Transactions on Geoscience and Remote Sensing*, http://dx.doi.org/10.1109/TGRS.2013.2272545.

Burkhalter, J. P., Martin, T. C., Allen, R. G., Kjaersgaard, J., Wilson, E., Alvarado, R., & Polly, J. S. (2013). Estimating crop water use via remote sensing techniques vs. conventional methods in the South Platte River Basin, Colorado. *Journal of the American Water Resources Association*, *49*, 498–517.

Burns, A. G., & Drici, W. (2011, June). Hydrology and water resources of Spring, Cave, Dry Lake, and Delamar valleys, Nevada and vicinity. *Presentation to the Office of the Nevada State Engineer: Southern Nevada Water Authority, Las Vegas, Nevada*.

Butson, C. R., & Fernandes, R. A. (2004). A consistency analysis of surface reflectance and leaf area index retrieval from overlapping clear-sky Landsat ETM+ imagery. *Remote Sensing of Environment*, *89*, 369–380.

Cammalleri, C., Anderson, M. C., Gao, F., Hain, C. R., & Kustas, W. P. (2013). A data fusion approach for mapping daily evapotranspiration at field scale. *Water Resources Research*, http://dx.doi.org/10.1002/wrcr.20349.

Cardille, J. A., White, J. C., Wulder, M.A., & Holland, T. (2012). Representative landscapes in the forested area of Canada. *Environmental Management*, *49*, 163–173.

Carpenter, S. R., DeFries, R., Dietz, T., Mooney, H. A., Polasky, S., Reid, W. V., & Scholes, R. J. (2006). Millennium ecosystem assessment: Research needs. *Ecology*, *314*, 257–258.

Carroll, M. L., Townshend, J. R., Dimiceli, C. M., Noojipady, P., & Sohlberg, R. A. (2009). A new global raster water mask at 250 m resolution. *International Journal of Digital Earth*, *2*(4), 291–308.

Chander, G., Markham, B.L., & Helder, D. L. (2009). Summary of current radiometric calibration coefficients for Landsat MSS, TM, ETM+, and EO-1 ALI sensors. *Remote Sensing of Environment*, *113*, 893–903.

Cohen, W. B., Zhiqiang, Y., & Kennedy, R. E. (2010). Detecting trends in forest disturbance and recovery using yearly Landsat time series: 2. TimeSync — Tools for calibration and validation. *Remote Sensing of Environment*, *114*, 2911–2924.

Czapla-Myers, J. S., Anderson, N. J., & Biggar, S. F. (2013). Early ground-based vicarious calibration results for Landsat 8 OLI. *Proceedings of SPIE*, *8866*.

Da Silva Curiel, A., Boland, L., Cooksley, J., Bekhti, M., Stephens, P., Sun, W., & Sweeting, M. (2005). First results from the disaster monitoring constellation (DMC). *Acta Astronautica*, *56*, 261–271.

Das, S. B., Joughin, I., Behn, M., Howat, I., King, M., Lizarraldi, D., & Bhatia, M. (2008). Fracture propagation to the base of the Greenland Ice Sheet during supraglacial lake drainage. *Science*, *320*, 778–781.

De Sy, V., Herold, M., Achard, F., Asner, G. P., Held, A., Kellndorfer, J., & Verbesselt, J. (2012). Synergies of multiple remote sensing data sources for REDD+ monitoring. *Current Opinion in Environmental Sustainability*, *4*, 696–706.

Debella-Gilo, M., & Kääb, A. (2011). Sub-pixel precision image matching for measuring surface displacements on mass movements using normalized cross-correlation. *Remote Sensing of Environment*, *115*, 130–142.

Dobson, J. E., Bright, E. A., Ferguson, R. L., Field, D. W., Wood, L. L., Haddad, K. D., Iredale, H., III, Jenson, J. R., Klemas, V. V., Orth, R. J., & Thomas, J. P. (1995). In D.O. Commerce (Ed.), *Coastal Change Analysis Program (C-CAP): guidance for regional implementation* (Seattle, WA).

Doraiswamy, P. C., Hatfield, J. L., Jackson, T. J., Akhmedov, B., Prueger, J., & Stern, A. (2004). Crop condition and yield simulations using Landsat and MODIS. *Remote Sensing of Environment*, *92*, 548–559.

Doraiswamy, P. C., Sinclair, T. R., Hollinger, S., Akhmedov, B., Stern, A., & Prueger, J. (2005). Application of MODIS derived parameters for regional crop yield assessment. *Remote Sensing of Environment*, *97*, 192–202.

Downing, J. A., Prairie, Y. T., Cole, J. J., Duarte, C. M., Tranvik, L. J., Striegl, R. G., McDowell, W. H., Kortelainen, P., Caraco, N. F., Melack, J. M., & Middelburg, J. J. (2006). The global abundance and size distribution of lakes, ponds, and impoundments. *Limnology and Oceanography*, *51*, 2388–2397.

Drusch, M., Del Bello, U., Carlier, S., Colin, O., Fernandez, V., Gascon, F., Hoersch, B., Isola, C., Laberinti, P., Martimort, P., Meygret, A., Spoto, F., Sy, O., Marchese, F., & Bargellini, P. (2012). Sentinel-2: ESA's Optical High-Resolution Mission for GMES Operational Services. *Remote Sensing of Environment*, *120*, 25–36.

Dubovik, O., Holben, B., Eck, T. F., Smirnov, A., Kaufman, Y. J., King, M.D., Tanre, D., & Slutsker, I. (2002). Variability of absorption and optical properties of key aerosol types observed in worldwide locations. *Journal of the Atmospheric Sciences*, *59*, 590–608.

Eidenshink, J., Schwind, B., Brewer, K., Zhu, Z. L., Quayle, B., & Howard, S. (2007). A project for monitoring trends in burn severity. *Fire Ecology*, *3*, 3–21.

ESA (2013). ESA-NASA collaboration fosters comparable land imagery. http://www.esa.int/Our_Activities/Observing_the_Earth/GMES/ESA_NASA_collaboration_fosters_comparable_land_imagery (Last accessed October 1st 2013)

Flanner, M. G., Shell, K. M., Barlage, M., Perovich, D. K., & Tschudi, M.A. (2011). Radiative forcing and albedo feedback from the Northern Hemisphere cryosphere between 1979 and 2008. *Nature Geoscience*, *4*, 151–155.

Food and Agriculture Organization (FAO) of the United Nations (2011). FAOSTAT/Resources/Land/. http://faostat3.fao.org/. (Last accessed October 1st 2013).

Fry, J. A., Xian, G., Jin, S., Dewitz, J. A., Homer, C. G., Yang, L., Barnes, C. A., Herold, N. D., & Wickham, J.D. (2011). Completion of the 2006 National Land Cover Database for the conterminous United States. *Photogrammetric Engineering and Remote Sensing*, *77*, 858–864.

Ganguly, S., Nemani, R. R., Zhang, G., Hashimoto, H., Milesi, C., Michaelis, A., Wang, W., Votava, P., Samanta, A., Melton, F., Dungan, J. L., Vermote, E., Gao, F., Knyazikhin, Y., & Myneni, R. B. (2012). Generating global Leaf Area Index from Landsat: Algorithm formulation and demonstration. *Remote Sensing of Environment*, *122*, 185–202.

GCOS (2004). Implementation Plan for the Global Observing System for Climate in Support of the UNFCCC, WMO/TD 1219. www.wmo.int/pages/prog/gcos/Publications/gcos-92_GIP.pdf

GCOS-154 (2011). Systematic observation requirements for satellite-based products for climate supplemental details to the satellite-based component of the implementation plan for the global observing system for climate in support of the UNFCCC - (2011 update). In A. Simmons (Ed.), GCOS-154 Geneva, Switzerland: United Nations Environment Programme, World Meteorological Organization and International Council for Science.

Gerace, A., & Schott, J. (2012, June 1). Over-water atmospheric correction for Landsat's new OLI sensor. *Proceeding of SPIE Ocean Sensing and Monitoring IV, 837211, Baltimore, Maryland*.

Gerace, A.D., Schott, J. R., & Nevins, R. (2013). Increased potential to monitor water quality in the near-shore environment with Landsat's next-generation satellite. *Journal of Applied Remote Sensing*, *7* (073558-073558).

Gitelson, A. A., Peng, Y., Masek, J. G., Rundquist, D. C., Verma, S., Suyker, A., Baker, J. M., Hatfield, J. L., & Meyers, T. (2012). Remote estimation of crop gross primary production with Landsat data. *Remote Sensing of Environment*, *121*, 404–414.

GOFC-GOLD (2012). A sourcebook of methods and procedures for monitoring and reporting anthropogenic greenhouse gas emissions and removals associated with deforestation, gains and losses of carbon stocks in forests remaining forests, and forestation. *GOFC-GOLD Report version COP18-1*. The Netherlands: GOFC-GOLD Land Cover Project Office, Wageningen University (219 pp.).

Gordon, H. R., & Clark, D. K. (1981). Clear water radiances for atmospheric correction of coastal zone color scanner imagery. *Applied Optics*, *20*, 4175–4180.

Goward, S., Arvidson, T., Williams, D., Faundeen, J., Irons, J., & Franks, S. (2006). Historical record of Landsat global coverage: Mission operations, NSLRSDA, and international cooperator stations. *Photogrammetric Engineering and Remote Sensing*, *72*, 1155–1169.

Goward, S. N., Masek, J. G., Williams, D. L., Irons, J. R., & Thompson, R. J. (2001). The Landsat 7 mission, Terrestrial research and applications for the 21st century. *Remote Sensing of Environment*, *78*, 3–12.

Griffiths, P., Kuemmerle, T., Kennedy, R. E., Abrudan, I. V., Knorn, J., & Hostert, P. (2012). Using annual time-series of Landsat images to assess the effects of forest restitution in post-socialist Romania. *Remote Sensing of Environment*, *118*, 199–214.

Gutman, G., Byrnes, R., Masek, J., Covington, S., Justice, C., Franks, S., & Headley, R. (2008). Towards monitoring Land-cover and land-use changes at a global scale: The global land survey. *Photogrammetric Engineering and Remote Sensing*, *74*, 6–10.

Hansen, J., Sato, M., & Ruedy, R. (2012). Perception of climate change. *Proceedings of the National Academy of Sciences of the United States of America*, *109*, E2415–E2423.

Hansen, M. C., Egorov, A., Potapov, P. V., Stehman, S. V., Tyukavina, A., Turubanova, S. A., Roy, D. P., Goetz, S. J., Loveland, T. R., Ju, J., Kommareddy, A., Kovalskyy, V., Forsythe, C., & Bents, T. (2014). Monitoring conterminous United States (CONUS) land cover change with Web-Enabled Landsat Data (WELD). *Remote Sensing of Environment*, *140*, 466–484.

Hansen, M. C., Egorov, A., Roy, D. P., Potapov, P., Ju, J., Turubanova, S., Kommareddy, I., & Loveland, T. R. (2011). Continuous fields of land cover for the conterminous United States using Landsat data: First results from the Web-Enabled Landsat Data (WELD) project. *Remote Sensing Letters*, *2*, 279–288.

Hansen, M. C., & Loveland, T. R. (2012). A review of large area monitoring of land cover change using Landsat data. *Remote Sensing of Environment*, *2012*, 66–74.

Hansen, M. C., Potapov, P. V., Moore, R., Hancher, M., Turubanova, S. A., Tyukavina, A., Thau, D., Stehman, S. V., Goetz, S. J., Loveland, T. R., Kommareddy, A., Egorov, A., Chini, L., Justice, C. O., & Townshend, J. R. G. (2013). High-resolution global maps of 21st-century forest cover change. *Science*, *342*(6160), 850–853.

Hansen, M. C., Roy, D. P., Lindquist, E., Adusei, B., Justice, C. O., & Altstatt, A. (2008). A method for integrating MODIS and Landsat data for systematic monitoring of forest cover and change in the Congo Basin. *Remote Sensing of Environment*, *112*(5), 2495–2513.

Helder, D., Thome, K. J., Mishra, N., Chander, G., Xiong, X., Angal, A., & Taeyoung, C. (2013). Absolute radiometric calibration of Landsat using a pseudo invariant calibration site. *IEEE Transactions on Geoscience and Remote Sensing*, *51*, 1360–1369.

Horler, D. N., & Ahern, F. J. (1986). Forestry information content of thematic mapper data. *International Journal of Remote Sensing*, *7*, 405–428.

Huang, C., Goward, S. N., Masek, J. G., Thomas, N., Zhu, Z., & Vogelmann, J. E. (2010). An automated approach for reconstructing recent forest disturbance history using dense Landsat time series stacks. *Remote Sensing of Environment*, *114*, 183–198.

INPE (2013). http://www.obt.inpe.br/prodes/index.php (Last accessed October 1st 2013)

IPCC (2013). Working Group I contribution to the IPCC Fifth Assessment Report Climate Change 2013. *The Physical Science Basis, Final Draft Underlying Scientific-Technical Assessment* (http://www.ipcc.ch/report/ar5/wg1/ (Last accessed October 1st 2013)).

Irons, J. R., Dwyer, J. L., & Barsi, J. A. (2012). The next Landsat satellite: The Landsat Data Continuity Mission. *Remote Sensing of Environment*, *122*, 11–21.

Irons, J. R., & Loveland, T. R. (2013). Eighth Landsat satellite becomes operational. *Photogrammetric Engineering and Remote Sensing*, *79*, 398–401.

Irons, J. R., & Masek, J. G. (2006). Requirements for a Landsat Data Continuity Mission. *Photogrammetric Engineering and Remote Sensing*, *72*, 1102–1108.

Jennings, M.D. (2000). Gap analysis: Concepts, methods, and recent results. *Landscape Ecology*, *15*, 5–20.

Johnson, D.M. (2008). A comparison of coincident Landsat-5 TM and Resourcesat-1 AWiFS imagery for classifying croplands. *Photogrammetric Engineering & Remote Sensing*, *74*, 1413–1423.

Johnson, D.M., & Mueller, R. (2010). The 2009 Cropland Data Layer. *Photogrammetric Engineering and Remote Sensing*, *76*, 1202–1205.

Ju, J., & Roy, D. P. (2008). The availability of cloud-free Landsat ETM+ data over the conterminous United States and globally. *Remote Sensing of Environment*, *112*, 1196–1211.

Ju, J., Roy, D. P., Vermote, E., Masek, J., & Kovalskyy, V. (2012). Continental-scale validation of MODIS-based and LEDAPS Landsat ETM+ atmospheric correction methods. *Remote Sensing of Environment*, *122*, 175–184.

Justice, C. O., Bailey, G. B., Maiden, M. E., Rasool, S. I., Strebel, D. E., & Tarpley, J.D. (1995). Recent data and information system initiatives for remotely sensed measurements of the land surface. *Remote Sensing of Environment*, *51*, 235–244.

Justice, C., Townshend, J., Vermote, E., Masuoka, E., Wolfe, R., Saleous, N., Roy, D., & Morisette, J. (2002). An overview of MODIS Land data processing and product status. *Remote Sensing of Environment*, *83*, 3–15.

Justice, C. O., Vermote, E., Townshend, J., Defries, R., Roy, D. P., Hall, D., Salomonson, V., Privette, J., Riggs, G., Strahler, A., Lucht, W., Myneni, R., Knyazikhin, Y., Running, S., Nemani, R., Wan, Z., Huete, A., van Leeuwen, W., Wolfe, R., Giglio, L., Muller, J. -P., Lewis, P., & Barnsley, M. (1998). The Moderate Resolution Imaging Spectroradiometer (MODIS): Land remote sensing for global change research. *IEEE Transactions on Geoscience and Remote Sensing*, *36*, 1228–1249.

Kalma, J.D., McVicar, T. R., & McCabe, M. F. (2008). Estimating land surface evaporation: A review of methods using remotely sensing surface temperature data. *Survey Geophysics*, http://dx.doi.org/10.1007/s10712-10008-19037-z.

Kaufman, Y. J. (1989). The atmospheric effect on remote sensing and its correction. In G. Asrar (Ed.), *Theory and Application of Optical Remote Sensing* (pp. 341). New York: Wiley-Interscience.

Keeling, C. D. (1998). Rewards and penalties of monitoring the earth. *Annual Review of Energy and the Environment*, *23*, 25–82.

Kennedy, R. E., Yang, Z., & Cohen, W. B. (2010). Detecting trends in forest disturbance and recovery using yearly Landsat time series: 1. LandTrendr — Temporal segmentation algorithms. *Remote Sensing of Environment*, *114*, 2897–2910.

Kennedy, R. E., Zhiqiang, Y., Cohen, W. B., Pfaff, E., Braaten, J., & Nelson, P. (2012). Spatial and temporal patterns of forest disturbance and regrowth within the area of the Northwest Forest Plan. *Remote Sensing of Environment*, *122*, 117–133.

Kieffer, H. H., Stone, T. C., Barnes, R. A., Bender, S.C., Eplee, R. E., Mendenhall, J. A., et al. (2003). On-orbit radiometric calibration over time and between spacecraft using the moon. *Proceedings of SPIE*, *4881*, 287–298.

Kovalskyy, V., & Roy, D. P. (2013). The global availability of Landsat 5 TM and Landsat 7 ETM+ land surface observations and implications for global 30 m Landsat data product generation. *Remote Sensing of Environment*, *130*, 280–293.

Kovalskyy, V., Roy, D. P., Zhang, X., & Ju, J. (2011). The suitability of multi-temporal Web-Enabled Landsat Data (WELD) NDVI for phenological monitoring — a comparison with flux tower and MODIS NDVI. *Remote Sensing Letters*, *3*(4), 325–334.

Lauer, D. T., Morain, S. A., & Salomonson, V. V. (1997). The Landsat program: Its origins, evolution, and impacts. *Photogrammetric Engineering and Remote Sensing*, *63*, 831–838.

Lee, D. S., Storey, J. C., Choate, M. J., & Hayes, R. (2004). Four years of Landsat-7 on-orbit geometric calibration and performance. *IEEE Transactions on Geoscience and Remote Sensing*, *42*, 2786–2795.

Lehmann, E. A., Wallace, J. F., Caccetta, P. A., Furby, S. L., & Zdunic, K. (2013). Forest cover trends from time series Landsat data for the Australian continent. *International Journal of Applied Earth Observation and Geoinformation*, *21*, 453–462.

Lehner, B., & Döll, P. (2004). Development and validation of a global database of lakes, reservoirs and wetlands. *Journal of Hydrology*, *296*, 1–22.

Lewis, P., Gómez-Dans, J., Kaminski, T., Settle, J., Quaife, T., Gobron, N., Styles, J., & Berger, M. (2012). An Earth Observation Land Data Assimilation System (EO-LDAS). *Remote Sensing of Environment*, *120*, 219–235.

Li, F., Jupp, D. L., Reddy, S., Lymburner, L., Mueller, N., Tan, P., & Islam, A. (2010). An evaluation of the use of atmospheric and BRDF correction to standardize Landsat data. *IEEE Journal of Selected Topics in Applied Earth Observations and Remote Sensing*, *3*, 257–270.

Li, J., & Sheng, Y. (2012). An automated scheme for glacial lake dynamics mapping using Landsat imagery and digital elevation models: A case study in the Himalayas. *International Journal of Remote Sensing*, *33*, 5194–5213.

Lindquist, E., Hansen, M. C., Roy, D. P., & Justice, C. O. (2008). The suitability of decadal image data sets for mapping tropical forest cover change in the Democratic Republic of Congo: Implications for the mid-decadal global land survey. *International Journal of Remote Sensing*, *29*, 7269–7275.

Lobell, D. B., Ortiz-Monasterio, J. I., Asner, G. P., Naylor, R. L., & Falcon, W. P. (2005). Combining field surveys, remote sensing, and regression trees to understand yield variations in an irrigated wheat landscape. *Agronomy Journal*, *97*, 241–249.

Loveland, T. R., & Dwyer, J. L. (2012). Landsat: Building a strong future. *Remote Sensing of Environment*, *122*, 22–29.

MacDonald, R. B., Hall, F. G., & Erb, R. B. (1976, Oct. 6–10). The use of Landsat data in a Large Area Crop Inventory Experiment (LACIE). *Proceedings of the Tenth International Symposium of Remote Sensing of Environment, Volume I (Ann Arbor, Michigan)*.

Mankoff, K. D., Jacobs, S. S., Tulaczyk, S. M., & Stammerjohn, S. (2012). The role of Pine Island Glacier ice shelf basal channels in deep-water upwelling, polynyas, and ocean circulation in Pine Island Bay, Antarctica. *Annals of Glaciology*, *53*, 123–128.

Markham, B.L., Dabney, P. W., Storey, J. C., Morfitt, R., Knight, E. J., Kvaran, G., & Lee, K. (2008, November 18-20). Landsat Data Continuity Mission calibration and validation. *Proceedings of the PECORA 17 Conference*.

Markham, B.L., Goward, S., Arvidson, T., Barsi, J., & Scaramuzza, P. (2006). Landsat-7 long-term acquisition plan radiometry — Evolution over time. *Photogrammetric Engineering & Remote Sensing*, *72*, 1129–1135.

Markham, B.L., & Helder, D. L. (2012). Forty-year calibrated record of earth-reflected radiance from Landsat: A review. *Remote Sensing of Environment*, *122*, 30–40.

Markham, B.L., Irons, J. R., & Storey, J. C. (2013). Landsat data continuity mission (LDCM) — Now Landsat-8: Six months on-orbit. *Proceedings of SPIE*, *8866*.

Markham, B.L., Storey, J. C., Williams, D. L., & Irons, J. R. (2004). Landsat sensor performance: History and current status. *IEEE Transactions on Geoscience and Remote Sensing, 42*, 2691–2694.

Masek, J. G., Goward, S. N., Kennedy, R. E., Cohen, W. B., Moisen, G. G., Schleeweis, K., & Huang, C. (2013). United States forest disturbance trends observed using Landsat time series. *Ecosystems, 16*, 1087–1104.

Masek, J. G., Vermote, E. F., Saleous, N. E., Wolfe, R., Hall, F. G., Huemmrich, K. F., Gao, F., Kutler, J., & Lim, T. K. (2006). A Landsat surface reflectance dataset for North America 1990–2000. *IEEE Geoscience and Remote Sensing Letters, 3*, 68–72.

Masuoka, E., Roy, D. P., Wolfe, R., Morisette, J., Sinno, S., Teague, M., Saleous, N., Devadiga, S., Justice, C., & Nickeson, J. (2011). MODIS land data products—Generation, quality assurance and validation. In B. Ramachandran, C. Justice, & M. Abrams (Eds.), *Land remote sensing and global environmental change: NASA's Earth observing system and the science of ASTER and MODIS. Remote Sensing and Digital Image Processing Series, Vol. 11*, Springer (873 pp.).

Mayaux, P., Pekel, J. F., Desclée, B., Donnay, F., Lupi, A., Achard, F., Clerici, M., Bodart, C., Brink, A., Nasi, R., & Belward, A. (2013). State and evolution of the African rainforests between 1990 and 2010. *Philosophical Transactions of the Royal Society, B: Biological Sciences, 368*(1625).

McCorkel, J., Thome, K., & Lockwood, R. B. (2013). Absolute radiometric calibration of narrow-swath imaging sensors with reference to non-coincident wide-swath sensors. *IEEE Transactions on Geoscience and Remote Sensing, 51*, 1309–1318.

Meybeck, M. (1995). Global distribution of lakes. In A. Lerman, D.M. Imboden, & J. R. Gat (Eds.), *Physics and chemistry of lakes* (pp. 1–35). Berlin: Springer-Verlag.

Miller, H. M., Richardson, Leslie, Koontz, S. R., Loomis, John, & Koontz, Lynne (2013). Users, uses, and value of Landsat satellite imagery—Results from the 2012 survey of users. *U.S. Geological Survey Open-File Report 2013–1269*, http://dx.doi.org/10.3133/ofr20131269 (51 pp.).

Mora, B., Wulder, M.A., White, J. C., & Hobart, G. (2013). Modeling stand height, volume, and biomass from very high spatial resolution satellite imagery and samples of airborne-lidar. *Remote Sensing, 5*, 2308–2326.

Motyka, R. J., Hunter, L., Echelmeyer, K., & Connor, C. (2003). Submarine melting at the terminus of a temperate tidewater glacier, LeConte Glacier, Alaska, USA. *Annals of Glaciology, 36*, 57–65.

Myhre, G., Kvalevag, M. M., & Schaaf, C. B. (2005). Radiative forcing due to anthropogenic vegetation change based on MODIS surface albedo data set. *Geophysical Research Letters, 32*, L21410, http://dx.doi.org/10.1029/2005GL024004.

Myneni, R., Tucker, C., Asrar, G., & Keeling, C. (1998). Interannual variations in satellite-sensed vegetation index data from 1981 to 1991. *Journal of Geophysical Research, 103*, 6145–6160.

Nemani, R., Hashimoto, H., Votava, P., Melton, F., Wang, W., Michaelis, A., Mutch, L., Milesi, C., Hiatt, S., & White, M. (2009). Monitoring and forecasting ecosystem dynamics using the Terrestrial Observation and Prediction System (TOPS). *Remote Sensing of Environment, 113*, 1497–1509.

Nemani, R., Votava, P., Michaelis, A., Melton, F., & Milesi, C. (2011). NASA Earth Exchange: A collaborative supercomputing environment for global change science. *Transaction of EOS, 13*, 109–110.

NRC, National Research Council (2000). *Issues in the Integration of Research and Operational Satellite Systems for Climate Research: Part I. Requirements and capabilities.* Washington D.C.: The National Academies Press (152 pp.).

NRC, National Research Council (2007). *Earth science and applications from space: Imperatives for the next DECADE AND BEYOND.* Washington DC: National Research Council (456 pp.).

NRC, National Research Council (2013). *Landsat and beyond: Sustaining and enhancing the nation's land imaging program.* Washington, DC: The National Academies Press (73 pp.).

NSEO (The Office of the State Engineer of the State of Nevada) (2012). *The Ruling (#6164) in the matter of applications 54003 through 54021, inclusive, filed to appropriate the underground waters of the Spring Valley hydrographic basin (184).* Nevada: Lincoln and White Pine Counties (218 pp.).

Olmanson, L. G., Bauer, M. E., & Brezonik, P. L. (2008). A 20-year Landsat water clarity census of Minnesota's 10,000 lakes. *Remote Sensing of Environment, 112*, 4086–4097.

Onderka, M., & Pekárová, P. (2008). Retrieval of suspended particulate matter concentrations in the Danube River from Landsat ETM data. *Science of the Total Environment, 397*, 238–243.

Quattrochi, D. A., & Luvall, J. C. (Eds.). (2004). *Thermal remote sensing in land surface processes.* Boca Raton, FL: CRC Press (440 pp.).

Rollins, M. G. (2009). LANDFIRE: A nationally consistent vegetation, wildland fire, and fuel assessment. *International Journal of Wildland Fire, 18*, 235–249.

Roy, D. P. (2000). The impact of misregistration upon composited wide field of view satellite data and implications for change detection. *IEEE Transactions on Geoscience and Remote Sensing, 38*, 2017–2032.

Roy, D. P., Borak, J. S., Devadiga, S., Wolfe, R. E., Zheng, M., & Descloitres, J. (2002). The MODIS Land product quality assessment approach. *Remote Sensing of Environment, 83*, 62–76.

Roy, D. P., Ju, J., Kline, K., Scaramuzza, P. L., Kovalskyy, V., Hansen, M. C., Loveland, T. R., Vermote, E. F., & Zhang, C. (2010). Web-enabled Landsat Data (WELD): Landsat ETM+ Composited Mosaics of the Conterminous United States. *Remote Sensing of Environment, 114*, 35–49.

Roy, D. P., Qin, Y., Kovalskyy, V., Vermote, E. F., Ju, J., Egorov, A., Hansen, M. C., Kommareddy, I., & Yan, L. (2014). Conterminous United States demonstration and characterization of MODIS-based Landsat ETM+ atmospheric correction. *Remote Sensing of Environment, 140*, 433–449.

Santos, C., Lorite, I. J., Allen, R. G., & Tasumi, M. (2012). Aerodynamic parameterization of the satellite-based energy balance (METRIC) Model for ET estimation in rainfed olive orchards of Andalusia, Spain. *Water Resources Management, 26*, 3267–3283.

Scambos, T. A., Bohlander, J. A., Shuman, C. A., & Skvarca, P. (2004). Glacier acceleration and thinning after ice shelf collapse in the Larsen B embayment, Antarctica. *Geophysical Research Letters, 31*(18), L18402.

Scambos, T. A., Dutkiewitcz, M. J., Wilson, J. C., & Bindschadler, R. A. (1992). Application of image cross-correlation software to the measurement of glacier velocity using satellite image data. *Remote Sensing of Environment, 42*, 177–186.

Scaramuzza, P. L., Bouchard, M.A., & Dwyer, J. L. (2012). Development of the Landsat data continuity mission cloud-cover assessment algorithms. *IEEE Transactions on Geoscience and Remote Sensing, 50*, 1140–1153.

Schaaf, C. B., Cihlar, J., Belward, A., Dutton, E., & Verstraete, M. (2009, May). Albedo and reflectance anisotropy. In R. Sessa (Ed.), *ECV-T8: GTOS assessment of the status of the development of standards for the terrestrial essential climate variables*. Rome: FAO.

Schaaf, C., Gao, F., Strahler, A. H., Lucht, W., Li, X., Tsang, T., Strugnell, N. C., Zhang, X., Jin, Y., Muller, J. -P., Lewis, P., Barnsley, M., Hobson, P., Disney, M., Roberts, G., Dunderdale, M., Doll, C., d'Entremont, R., Hu, B., Liang, S., Privette, J. L., & Roy, D. P. (2002). First operational BRDF, albedo and nadir reflectance products from MODIS. *Remote Sensing of Environment, 83*, 135–148.

Schaaf, C. L. B., Liu, J., Gao, F., & Strahler, A. H. (2011). MODIS albedo and reflectance anisotropy products from aqua and terra. In B. Ramachandran, C. Justice, & M. Abrams (Eds.), *Land remote sensing and global environmental change: NASA's earch observing system and the science of ASTER and MODIS. Remote Sensing and Digital Image Processing Series, Vol. 11*, Springer (873 pp.).

Schott, J. R., Hook, S. J., Barsi, J. A., Markham, B.L., Miller, J., Padula, F. P., & Raqueno, N. G. (2012). Thermal infrared radiometric calibration of the entire Landsat 4, 5, and 7 archive (1982–2010). *Remote Sensing of Environment*, 41–49.

Schroeder, W., Prins, E., Giglio, L., Csiszar, I., Schmidt, C., Morisette, J., & Morton, D. (2008). Validation of GOES and MODIS active fire detection products using ASTER and ETM+ data. *Remote Sensing of Environment, 112*, 2711–2726.

Sheng, Y., & Li, J. (2011). Satellite-observed endorheic lake dynamics across the Tibetan Plateau between circa 1976 and 2000. In Y. Q. Wang (Ed.), *Remote sensing of protected lands* (pp. 305–319). New York: CRC Press.

Shimabukuro, Y. E., Batista, G. T., Mello, E. M. K., Moreira, J. C., & Duarte, V. (1998). Using shade fraction image segmentation to evaluate deforestation in Landsat Thematic Mapper images of the Amazon Region. *International Journal of Remote Sensing, 19*, 535–541.

Shuai, Y., Masek, J. G., Gao, F., & Schaaf, C. B. (2011). An algorithm for the retrieval of 30-m snow-free albedo from Landsat surface reflectance and MODIS BRDF. *Remote Sensing of Environment, 115*, 2204–2216.

Shukla, A., Arora, M. K., & Gupta, R. P. (2010). Synergistic approach for mapping debris-covered glaciers using optical–thermal remote sensing data with inputs from geomorphometric parameters. *Remote Sensing of Environment, 114*, 1378–1387.

Skole, D. S., Justice, C. O., Janetos, A., & Townshend, J. R. G. (1997). *A land cover change monitoring program: a strategy for international effort.* Mitigation and Adaptation Strategies for Global Change. Amsterdam, The Netherlands: Kluwer, 1–19.

Skole, D., & Tucker, C. (1993). Tropical deforestation and habitat fragmentation in the Amazon: Satellite data from 1978 to 1988. *Science, 260*, 1905–1910.

Slater, P. N., Biggar, S. F., Holm, R. G., Jackson, R. D., Mao, Y., Moran, M. S., Palmer, J. M., & Yuan, B. (1987). Reflectance-and radiance-based methods for the in-flight absolute calibration of multispectral sensors. *Remote Sensing of Environment, 22*, 11–37.

Sleeter, B.M., Sohl, T. L., Bouchard, M.A., Reker, R. R., Soulard, C. E., Acevedo, W., Griffith, G. E., Sleeter, R. R., Auch, R. F., Sayler, K. L., Prisley, S., & Zhu, Z. (2012). Scenarios of land use and land cover change in the conterminous United States: Utilizing the special report on emission scenarios at ecoregional scales. *Global Environmental Change, 22*, 896–914.

Smith, L. C., Sheng, Y., MacDonald, G. M., & Hinzman, L. D. (2005). Disappearing Arctic lakes. *Science, 308*(5727), 1429.

Soverel, N. O., Coops, N. C., White, J. C., & Wulder, M.A. (2010). Characterizing the forest fragmentation of Canada's national parks. *Environmental Monitoring and Assessment, 164*, 481–499.

Stearns, L., Smith, B., & Hamilton, G. (2008). Increased flow speed on a large Antarctic glacier caused by sub-glacial floods. *Nature Geoscience, 1*, 827–838.

Stoney, W. E. (2008). *ASPRS guide to land imaging satellites.* Noblis Inc. (15 pp. URL: http://www.asprs.org/a/news/satellites/ASPRS_DATABASE_021208.pdf (Last accessed October 1st 2013)).

Storey, J., Lee, K., & Choate, M. (2008, November 18–20). Geometric performance comparison between the OLI and the ETM+. *Proceedings of the PECORA 17 Conference.*

Sullivan, A., Huntington, J., & Morton, C. (2011). Remote sensing of consumptive use in the Walker River Basin, Nevada. *American Water Resource Association Annual Conference, Albuquerque, NM, 2011.*

SWBD (2005). Shuttle Radar Topography Mission water body data set. http://www2.jpl.nasa.gov/srtm/index.html (Digital Media (Last accessed October 1st 2013))

Swithinbank, C. (1988). Satellite image atlas of glaciers of the world: Antarctica. In R. S. Williams, & J. G. Ferrigno (Eds.), *U.S. Geological Survey Professional Paper 1386-B.*

Tackett, J. L., & Di Girolamo, L. (2009). Enhanced aerosol backscatter adjacent to tropical trade wind clouds revealed by satellite-based lidar. *Geophysical Research Letters, 36*, L14804.

Tedesco, M., & Steiner, N. (2011). In-situ multispectral and bathymetric measurements over a supraglacial lake in western Greenland using a remotely controlled watercraft. *The Cryosphere, 5*(2), 445–452.

Thome, K., Reuter, D., Lunsford, A., Montanaro, M., Smith, R., Tesfaye, Z., & Wenny, B. (2011). Calibration of the thermal infrared sensor on the Landsat Data Continuity

Mission. *Geoscience and Remote Sensing Symposium (IGARSS), 24–29 July 2011, 2011 IEEE International* (pp. 985–988).
Townshend, J. R. G., & Justice, C. O. (1988). Selecting the spatial-resolution of satellite sensors required for global monitoring of land transformations. *International Journal of Remote Sensing, 9*, 187–236.
Townshend, J. R. G., Justice, C. O., Gurney, C., & McManus, J. (1992). The impact of misregistration on change detection. *IEEE Transactions on Geoscience and Remote Sensing, 30*, 1054–1060.
Trenberth, K. E., Anthes, R. A., Belward, A., Brown, O., Habermann, T., Karl, T. R., Running, S., Ryan, B., Tanner, M., & Wielicki, B. (2013). Challenges of a sustained climate observing system. In G. R. Asrar, & J. W. Hurrell (Eds.), *Climate Science for Serving Society: Research, Modeling and Prediction Priorities*. Springer (484 pp.).
Trezza, R., Allen, R. G., Robison, C. W., Kramber, W., Kjaersgaard, J., Tasumi, M., & Garcia, M. (2008). Enhanced resolution of evapotranspiration from riparian systems and field edges by sharpening the Landsat thermal band. *Proceedings of the ASCE EWRI World Environmental & Water Resources Congress, May 12–16, 2008. Honolulu, Hawaii, USA* (9 pp.).
Tu, T. M., Huang, P.S., Hung, C. L., & Chang, C. P. (2004). A fast intensity-hue-saturation fusion technique with spectral adjustment for IKONOS imagery. *IEEE Geoscience and Remote Sensing Letters, 1*, 309–312.
Tucker, C. J., Grant, D.M., & Dykstra, J.D. (2004). NASA's global orthorectified Landsat data set. *Photogrammetric Engineering and Remote Sensing, 70*, 313–322.
Tucker, C. J., Pinzon, J. E., Brown, M. E., Slayback, D. A., Pak, E. W., Mahoney, R., Vermote, E. F., & El Saleous, N. (2005). An extended AVHRR 8-km NDVI dataset compatible with MODIS and SPOT vegetation NDVI data. *International Journal of Remote Sensing, 26*, 4485–4498.
U.S. Geological Survey (2007). *Facing tomorrow's challenges—U.S. Geological Survey science in the decade 2007–2017. U.S. Geological Survey Circular, 1309*, (70 pp.).
UN (2012). The future we want. *Outcome of the United Nations Conference on Sustainable Development, Rio de Janeiro, Brazil 20–22 June 2012, A/CONF.216/L* (pp. 53).
Ungar, S. G., Pearlman, J. S., Mendenhall, J. A., & Reuter, D. (2003). Overview of the Earth Observing One (EO-1) mission. *IEEE Transactions on Geoscience and Remote Sensing, 41*, 1149–1159.
United Nations Population Division (2011). *World population prospects: The 2010 revision.* New York: United Nations (http://esa.un.org/unpd/wpp/index.htm).
USDA, National Agricultural Statistics Service Cropland Data Layer (2013). *Published crop-specific data layer [Online].* Washington, DC: USDA-NASS (Available at http://nassgeodata.gmu.edu/CropScape/ (accessed 13.05.14)).
Ustin, S. L., Roberts, D. A., Gamon, J. A., Asner, G. P., & Green, R. O. (2004). Using imaging spectroscopy to study ecosystem processes and properties. *BioScience, 54*, 523–534.
Vermote, E. F., El Saleous, N. Z., & Justice, C. O. (2002). Atmospheric correction of MODIS data in the visible to middle infrared: first results. *Remote Sensing of Environment, 83*, 97–111.
Vermote, E. F., & Kotchenova, S. (2008). Atmospheric correction for the monitoring of land surfaces. *Journal of Geophysical Research, 113*, D23S90.
Vermote, E., Saleous, N. E. L., & Holben, B. (1995). Aerosol retrieval and atmospheric correction. In G. D'Souza, A. S. Belward, & J. P. Malingreau (Eds.), *Advances in the use of NOAA AVHRR data for land applications* (pp. 93–124). Springer.
Vogelmann, J. E., Kost, J. R., Tolk, B., Howard, S., Short, K., Chen, X. X., Huang, C. Q., Pabst, K., & Rollins, M. G. (2011). Monitoring landscape change for LANDFIRE using multitemporal satellite imagery and ancillary data. *IEEE Journal of Selected Topics in Applied Earth Observations and Remote Sensing, 4*, 252–264.
WELD (2013). WELD Version 1.5 Product Distribution Web Site. http://weld.cr.usgs.gov/ (Last accessed October 1st 2013)
Williams, R. S., Ferrigno, J. G., Swithinbank, C., Lucchitta, B. K., & Seekins, B.A. (1995). Coastal-change and glaciological maps of Antarctica. *Annals of Glaciology, 21*, 284–290.
Williams, D. L., Goward, S., & Arvidson, T. (2006). Landsat: yesterday, today, and tomorrow. *Photogrammetric Engineering & Remote Sensing, 72*(10), 1171–1178.
Wolfe, R., Nishihama, M., Fleig, A., Kuyper, J., Roy, D., Storey, J., & Patt, F. (2002). Achieving sub-pixel geolocation accuracy in support of MODIS land science. *Remote Sensing of Environment, 83*, 31–49.
Woodcock, C. E., Allen, R., Anderson, M., Belward, A., Bindschadler, R., Cohen, W. B., Gao, F., Goward, S. N., Helder, D., Helmer, E., Nemani, R., Oreopoulos, L., Schott, J., Thenkabail, P.S., Vermote, E. F., Vogelmann, J., Wulder, M.A., & Wynne, R. (2008). Free access to Landsat imagery. *Science, 320*, 1011.
Wu, X., Sullivan, J. T., & Heidinger, A. K. (2010). Operational calibration of the Advanced Very High Resolution Radiometer (AVHRR) visible and near-infrared channels. *Canadian Journal of Remote Sensing, 36*, 602–616.
Wulder, M.A., & Masek, J. G. (2012). Preface to Landsat Legacy Special Issue: Continuing the Landsat legacy. *Remote Sensing of Environment, 122*, 1.
Wulder, M.A., Masek, J. G., Cohen, W. B., Loveland, T. R., & Woodcock, C. E. (2012). Opening the archive: How free data has enabled the science and monitoring promise of Landsat. *Remote Sensing of Environment, 122*, 2–10.
Wulder, M.A., White, J. C., Cranny, M., Hall, R. J., Luther, J. E., Beaudoin, A., Goodenough, D.G., & Dechka, J. A. (2008). Monitoring Canada's forests. Part 1: Completion of the EOSD land cover project. *Canadian Journal of Remote Sensing, 34*, 549–562.
Wulder, M.A., White, J. C., Masek, J. G., Dwyer, J., & Roy, D. P. (2011). Continuity of Landsat observations: Short term considerations. *Remote Sensing of Environment, 115*, 747–751.
Xue, Y., Li, Y., Guang, J., Zhang, X., & Guo, X. (2008). Small satellite remote sensing and applications — History, current AND FUTURE. *International Journal of Remote Sensing, 29*, 4339–4372.
Yamaguchi, Y., Kahle, A.B., Tsu, H., Kawakami, K., & Pniel, M. (1998). Overview of Advanced Spaceborne Thermal Emission and Reflection Radiometer (ASTER). *IEEE Transactions on Geoscience and Remote Sensing, 36*, 1062–1071.
Zhu, Z., Woodcock, C. E., & Olofsson, P. (2012). Continuous monitoring of forest disturbance using all available Landsat imagery. *Remote Sensing of Environment, 122*, 75–91.
Zwally, H. J., Abdalati, W., Hering, T., Larson, K., Saba, J., & Steffen, K. (2002). Surface melt-induced acceleration of Greenland ice-sheet flow. *Science, 297*, 218–222.